

SAN/3042-4
FR-10064

AMORPHOUS SILICON SOLAR CELLS
BY HYDROGEN IMPLANTATION

Final Report
For the Period
1 January 1979 - 31 August 1980

A. R. Kirkpatrick and A. A. Melas
August 1980

Work Performed Under
Contract No. 03-79-ET-23042.000

For:
U. S. DEPARTMENT OF ENERGY
SOLAR ENERGY



DISCLAIMER

This report was prepared as an account of work sponsored by an agency of the United States Government. Neither the United States Government nor any agency thereof, nor any of their employees, makes any warranty, express or implied, or assumes any legal liability or responsibility for the accuracy, completeness, or usefulness of any information, apparatus, product, or process disclosed, or represents that its use would not infringe privately owned rights. Reference herein to any specific commercial product, process, or service by trade name, trademark, manufacturer, or otherwise does not necessarily constitute or imply its endorsement, recommendation, or favoring by the United States Government or any agency thereof. The views and opinions of authors expressed herein do not necessarily state or reflect those of the United States Government or any agency thereof.

DISCLAIMER

Portions of this document may be illegible in electronic image products. Images are produced from the best available original document.

SAN/3042-4
UC-63
FR-10064

AMORPHOUS SILICON SOLAR CELLS
BY HYDROGEN IMPLANTATION

FINAL REPORT
FOR THE PERIOD
1 January 1979 - 31 August 1980

A.R. Kirkpatrick and A.A. Melas

This report was prepared as an account of work sponsored by an agency of the United States Government. Neither the United States nor any agency thereof, nor any of their employees, makes any warranty, expressed or implied, or assumes any legal liability or responsibility for any third party's use or the results of such use of any information, apparatus, product or process disclosed in this report, or represents that its use by such third party would not infringe privately owned rights.

SPIRE CORPORATION
PATRIOTS PARK
BEDFORD, MA 01730

Prepared for the

U.S. DEPARTMENT OF ENERGY
SOLAR ENERGY
Under Contract No. 03-79-ET-23042.000

TABLE OF CONTENTS

| <u>Section</u> | | <u>Page</u> |
|----------------|--|-------------|
| 1 | INTRODUCTION | 1 |
| 2 | PROGRAM DISCUSSION | 3 |
| 2.1 | Planned Program | 3 |
| 2.2 | Implantation Requirements | 5 |
| 2.3 | Implantation Facilities and Procedures | 12 |
| 2.4 | Test Structures | 15 |
| 2.5 | Implantation Effects Investigation | 16 |
| 2.6 | Amorphous Cell Experiment | 37 |
| | 2.5.1 Material Modifications Studies | 16 |
| | 2.5.2 Device Characteristics Studies | 33 |
| | 2.6 Amorphous Cell Experiment | 37 |
| 3 | SUMMARY | 45 |

LIST OF FIGURES

| <u>Figure</u> | | <u>Page</u> |
|---------------|---|-------------|
| 1 | Approach to Amorphous Silicon Material and Devices by Ion Implantation | 4 |
| 2 | Predicted Stopping Distributions for 10, 50 and 200 keV $^1\text{H}^+$ | 6 |
| 3 | Predicted Stopping Distributions for 10 and 200 keV $^{11}\text{B}^+$ | 7 |
| 4 | Predicted Stopping Distributions for 10 and 200 keV $^{19}\text{F}^+$ | 8 |
| 5 | Predicted Stopping Distributions for 10 and 200 keV $^{28}\text{Si}^+$ | 9 |
| 6 | Predicted Stopping Distributions for 10 and 200 keV $^{31}\text{P}^+$ | 10 |
| 7 | Throughput Versus Beam Current for Silicon Film Modification Processes | 11 |
| 8 | Cooled Sample Holder for Special Implantations | 13 |
| 9 | Wafer Temperature Versus Implant Time as Function of Ion Beam Energy Input | 14 |
| 10 | Cell Device Test Structure | 17 |
| 11 | Illuminated Output Characteristics of Nine Polysilicon Cell Devices on Test Structure | 18 |
| 12 | $^{28}\text{Si}^+$ Implants Used for Amorphization of Polysilicon Film | 20 |
| 13 | Transmittance Versus Wavelength of 0.5 μm Silicon Film Amorphized by $^{28}\text{Si}^+$ Implant | 21 |
| 14 | Predicted Distribution of Hydrogen in Silicon From Combined 12, 20 and 30 keV $^1\text{H}^+$ Implants | 23 |
| 15 | Transmittance Versus Wavelength of 0.5 μm Silicon Film Implanted with 3×10^{16} $^1\text{H}^+$ Ions/cm ² | 24 |

LIST OF FIGURES (Concluded)

| | | |
|----|--|----|
| 16 | Transmittance Versus Wavelength of 0.5 μm Silicon Film Implanted with 1×10^{17} $^1\text{H}^+$ Ions/ cm^2 | 25 |
| 17 | Transmittance Versus Wavelength of 0.5 μm Silicon Film Implanted with 3×10^{17} $^1\text{H}^+$ Ions/ cm^2 | 26 |
| 18 | Transmittance Versus Wavelength of 0.5 μm Silicon Film Implanted with 3×10^{16} $^1\text{H}^+$ Ions/ cm^2 and Amorphized by $^{28}\text{Si}^+$ Implants | 27 |
| 19 | Transmittance Versus Wavelength of 0.5 μm Silicon Film Implanted with 3×10^{17} $^1\text{H}^+$ Ions/ cm^2 and Amorphized by $^{28}\text{Si}^+$ Implant | 28 |
| 20 | Relative Infrared Transmittance Versus Wavenumber From Silicon Films on Silicon Wafer Substrates | 29 |
| 21 | AM0 Current Density Versus Voltage of 0.1 cm^2 Device Implanted with 1×10^{17} $^1\text{H}^+$ ions/ cm^2 | 34 |
| 22 | AM0 Current Density Versus Voltage of 0.1 cm^2 Device with Amorphizing $^{28}\text{Si}^+$ Implant | 35 |
| 23 | AM0 Current Density Versus Voltage Characteristics of 0.1 cm^2 Device with $^1\text{H}^+$ and $^{28}\text{Si}^+$ Implants | 36 |
| 24 | Amorphous Silicon Cell Structure | 38 |
| 25 | Current-Voltage Characteristics of 2x2 cm Test Cells | 40 |
| 26 | I-V Characteristics of Unstable Test Cell | 41 |
| 27 | Bias Voltage at Constant Current of Unstable Test Cell | 42 |

SECTION 1 INTRODUCTION

An investigation has been conducted to ascertain whether ion implantation can play a practical role in the preparation of amorphous silicon semiconductor material films and solar cell devices. The title of the program performed has been "Amorphous Silicon Solar Cells by Hydrogen Implantation". The prospective applications of implantation which have been considered have not been limited only to introduction of the hydrogen needed for hydrogenated amorphous silicon materials. Much broader utilization of implantation has been examined and found to be feasible. Relative to fabrication of amorphous solar cell materials and devices, it is reasonable to consider implantation for hydrogenation, for structural amorphization and for incorporation of common dopant impurities or other functional constituents.

As a processing technique, ion implantation is undergoing radical changes relative to the scope of applications for which it is being used or is planned for use in the future. This change is occurring primarily because of rapid advances in machine technology. Available beam currents have increased from tenths of milliamperes which were available only a few years ago to levels which may soon approach the 100 milliampere range and special purpose implanters to deliver amperes are under consideration. As beam currents have increased it has become apparent that implantation need no longer be limited to low dose doping operations or even to use only by the semiconductor industry — implantation is becoming a powerful tool for general modification of surfaces.

Significant limitation effects do exist and cannot be ignored, but within limits defined by fundamental physics, implantation in combination with specialized annealing procedures can be looked upon as a powerful tool for almost arbitrarily definable adjustment of material composition and structure in the vicinity of a surface. The distance range over which implantation can be employed for these purposes is severely restricted but in the case an amorphous silicon solar cell, implantation range can be adequate to address the entire device structure.

Under the program which has been conducted, possible approaches to utilizing implantation in the preparation of materials adequate for amorphous silicon solar cells have been investigated. Concurrent investigations to develop an approach to employing implantation effectively in the total fabrication of amorphous silicon solar cells have been performed. Procedures for controlled, selectable modification of material characteristics have been sought. Some amorphous silicon cell devices have been fabricated but detailed knowledge of the material and structural characteristics needed in a practical cell remain to be adequately identified.

SECTION 2 PROGRAM DISCUSSION

2.1 PLANNED PROGRAM

Under the program performed, several prospective applications of ion implantation to preparation of amorphous materials and to formation of device component elements for amorphous silicon solar cells have been considered. The program has been addressed toward validating technical feasibility of possibilities suggested in Figure 1. In principle ion implantation, in conjunction with adequate annealing techniques when required, can allow very broad adjustments to be made to composition and microphysical structure of a silicon film adequately thick to meet requirements of an amorphous cell. If implantation can be fully exploited by such an approach, starting material for an amorphous cell could be a silicon film which would not necessarily be initially amorphous or include required dopants and compositional constituents such as hydrogen. A series of selected implantation procedures could be used to accomplish the following:

- Doping
- Hydrogenation
- Amorphization
- Special impurity incorporation

In order to evaluate the validity and merit of the candidate applications of implantation, the program performed was to include the following:

- (i) Examination of implantation limits and requirements
- (ii) Development of adequate experimental implantation capabilities and procedures
- (iii) Development of a material test structure and of an amorphous solar cell test structure
- (iv) Preliminary survey of implantation effect upon silicon film material and device structures
- (v) Preparation of an amorphous silicon cell

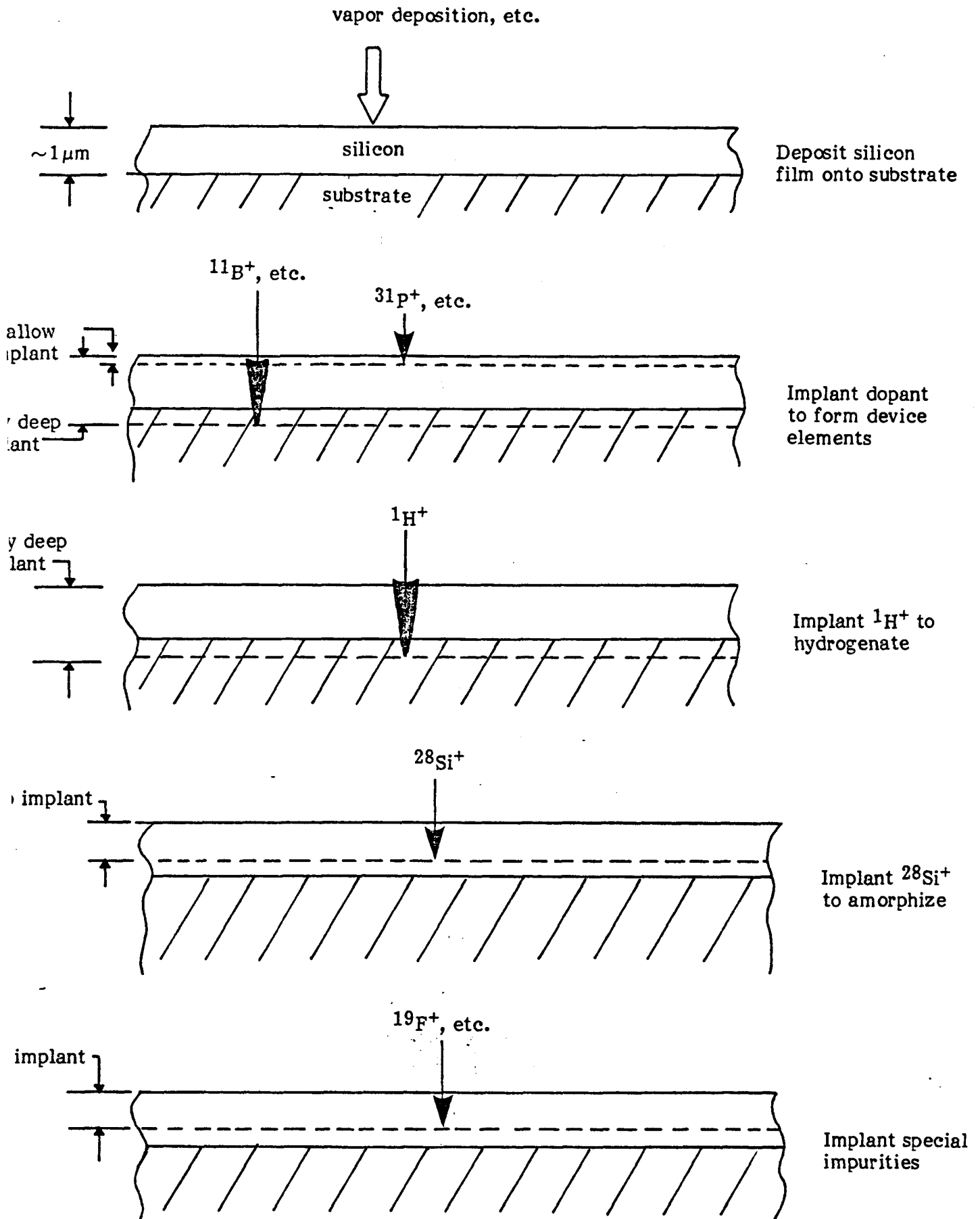


FIGURE 1. APPROACH TO AMORPHOUS SILICON MATERIAL AND DEVICES BY ION IMPLANTATION

2.2 IMPLANTATION REQUIREMENTS

If ion implantation is to be employed effectively in the preparation of amorphous silicon materials and amorphous silicon solar cells, several ion species must be introduced into a silicon film in satisfactory distributions. Although a problem exists in that information needed to allow distributions of all constituents for the amorphous silicon cell to be adequately defined is not presently available, it is possible to examine the range of conditions which can be considered. Existing production implantation machines can be built to operate at ion energies from less than 10 keV up to 200 keV or more. It is reasonable to assume similar energies can be delivered by much higher throughput implanters which will be designed in the future. Figures 2 through 6 show example 10 and 200 keV expected stopping distributions in silicon for $^1\text{H}^+$, $^{11}\text{B}^+$, $^{19}\text{F}^+$, $^{28}\text{Si}^+$ and $^{31}\text{P}^+$ ions. The 200 keV implant profiles suggest maximum depths to which given ions might be easily introduced by implantation. Of particular interest is the observation that proton implantation could be used to hydrogenate silicon layers to a depth of more than 2 micrometers.

Standard applications of ion implantation by the semiconductor industry have been those involving introduction of dopants to form device elements such as MOS gates, junctions, etc. Required ion fluence levels have been in the range 10^{11} through 10^{16} ions/cm². If much broader material modification roles are to be assigned to implantation, some of the fluence levels involved could be substantially higher. To eliminate crystalline order of a silicon surface layer requires approximately 10^{16} ions/cm². Background conductivity type doping of a 1 micrometer thick film or formation of a junction layer could also require up to 10^{16} ions/cm². Implant levels necessary to introduce hydrogen or other major constituent to form silicon alloys depend upon fractional composition level desired but will range up to 10^{18} ions/cm² for approximately 20 percent composition of implanted component in a 1 micrometer thick film.

Production implanters now available have not been designed for processes which demand dose levels as high as those which could be required for hydrogenation or introduction of a major constituent and at the same time must be performed at high processed area throughput rates. If they will be used, such machines can be developed. Figure 7 shows throughput rate versus usable implanter beam current for procedures of interest for amorphous silicon cells. It is evident from the figure that existing implanters can be adequate for research and development of amorphous materials applications, but beam currents of amperes or more will be needed from production units if they are to provide compositional implants.

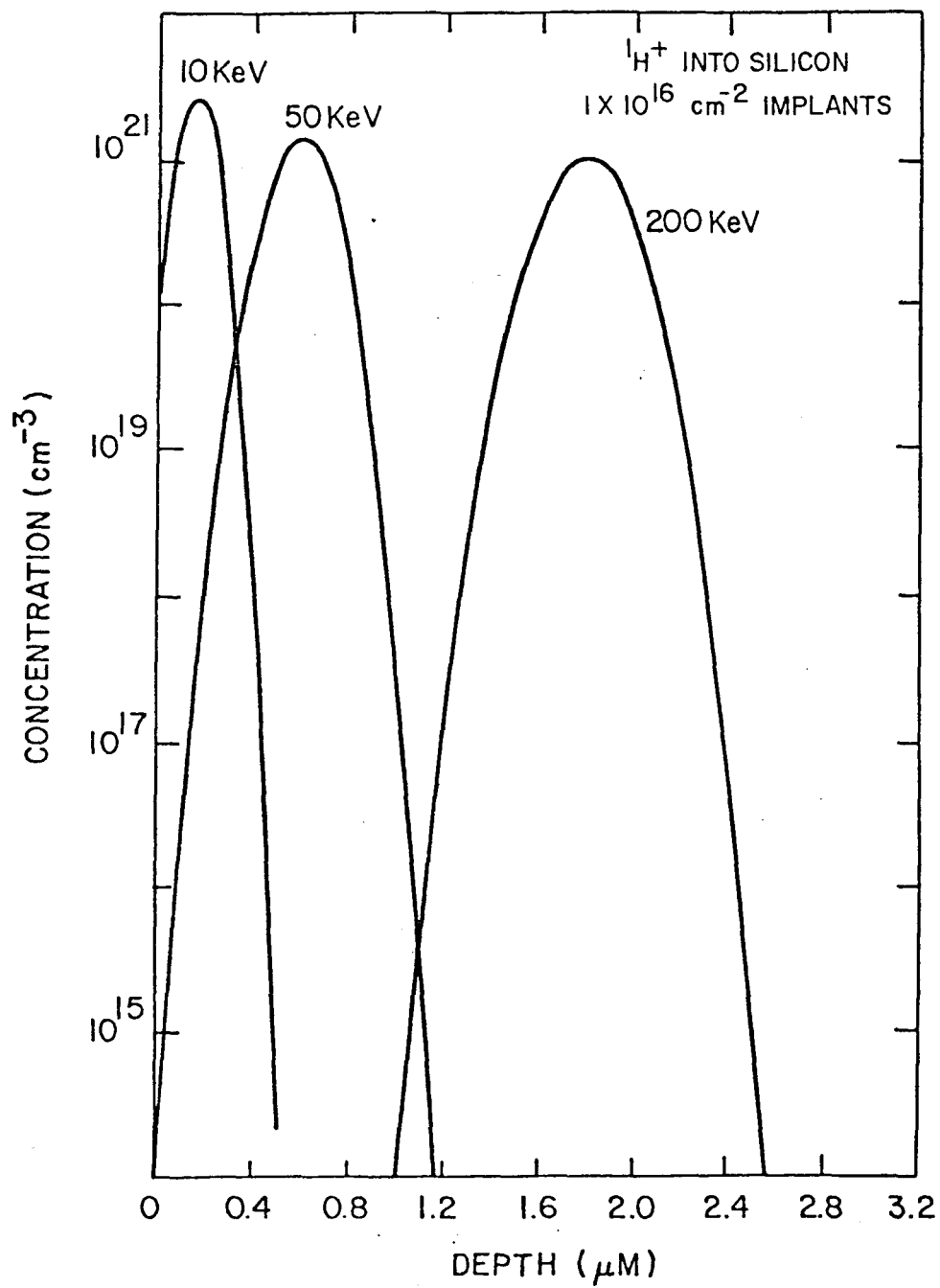


FIGURE 2. PREDICTED STOPPING DISTRIBUTIONS FOR 10, 50 AND 200 keV ${}^1\text{H}^+$

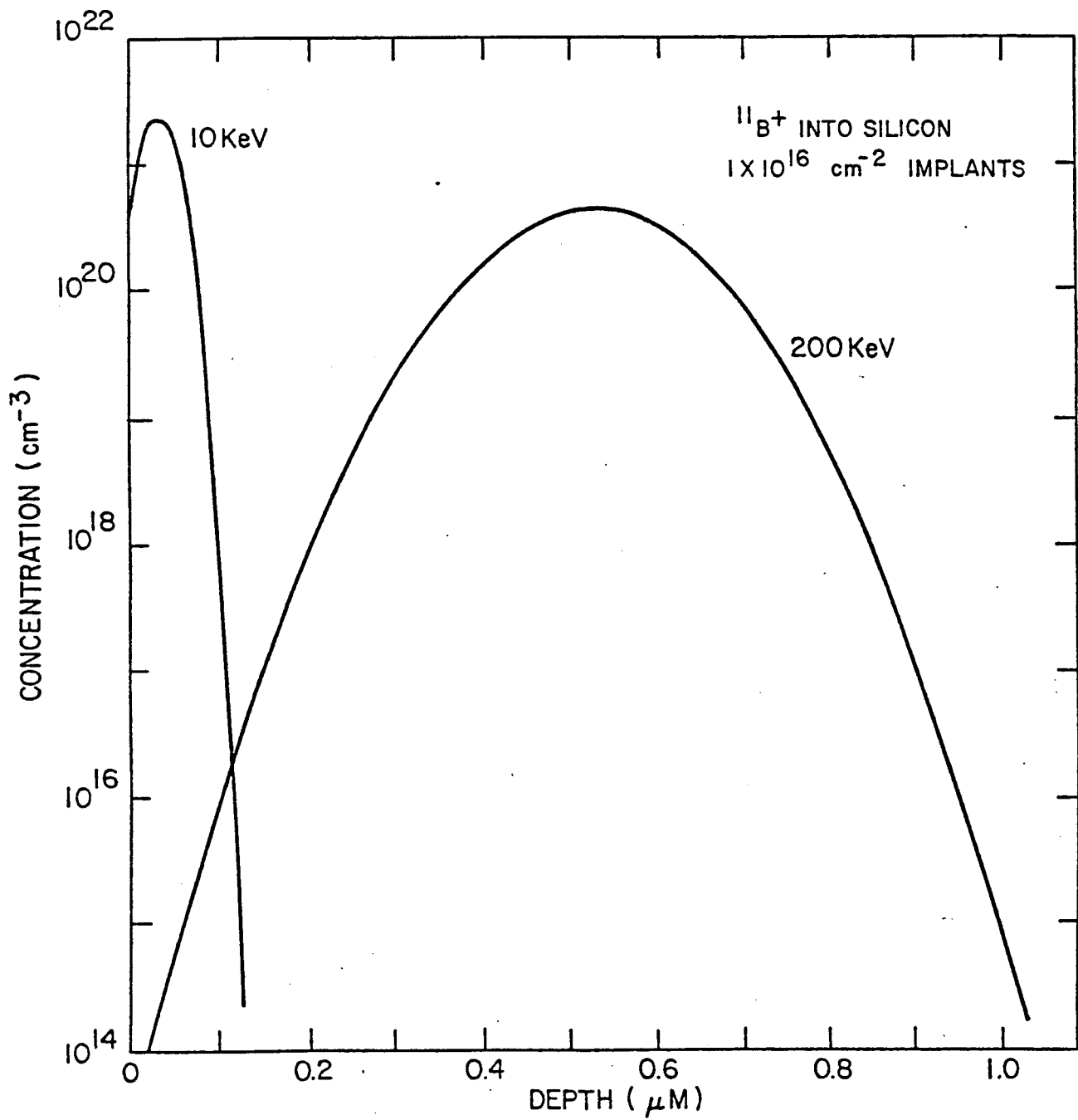


FIGURE 3. PREDICTED STOPPING DISTRIBUTIONS FOR 10 AND 200 keV ¹¹B⁺

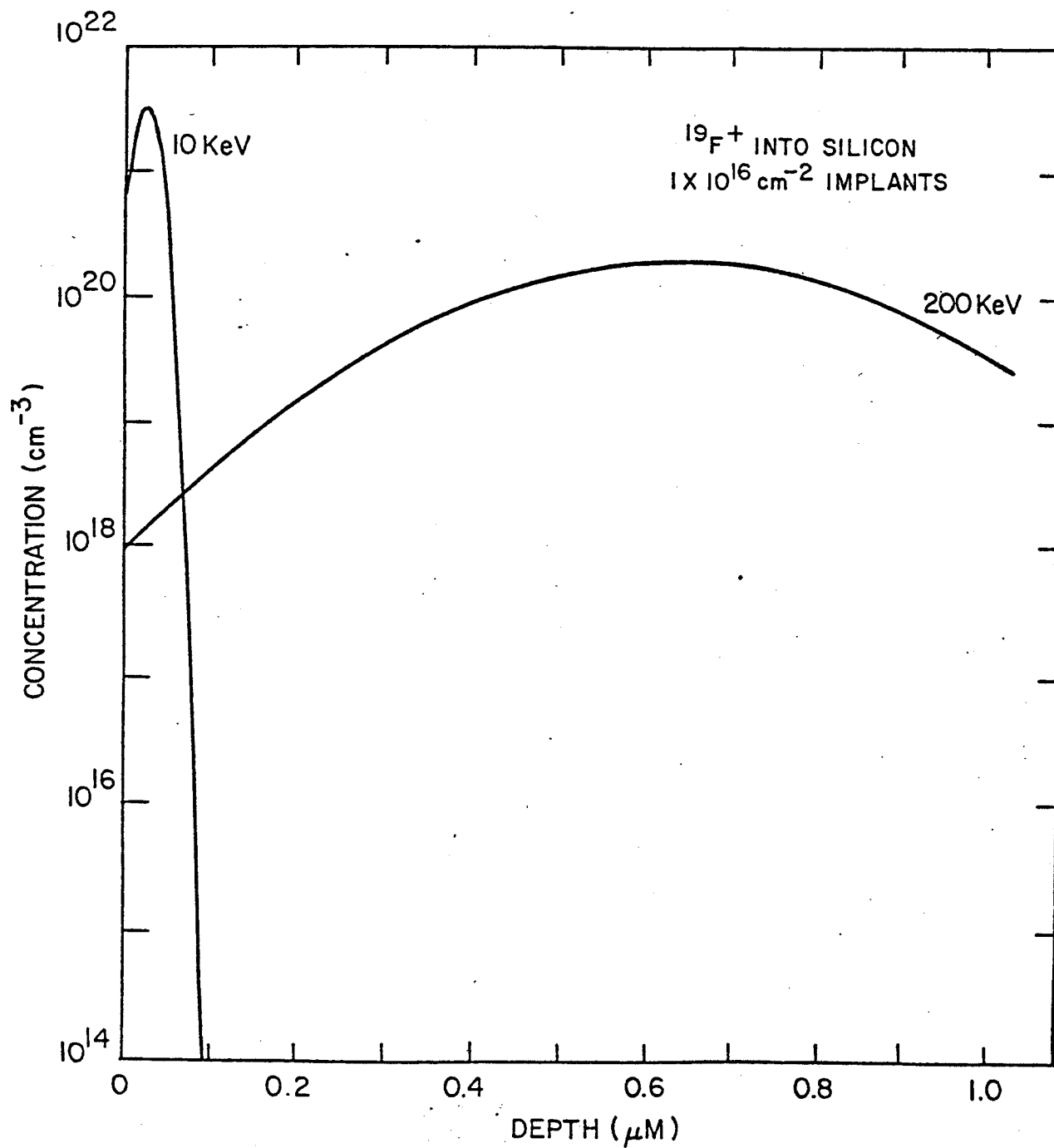


FIGURE 4. PREDICTED STOPPING DISTRIBUTIONS FOR 10 AND 200 keV $^{19}\text{F}^+$

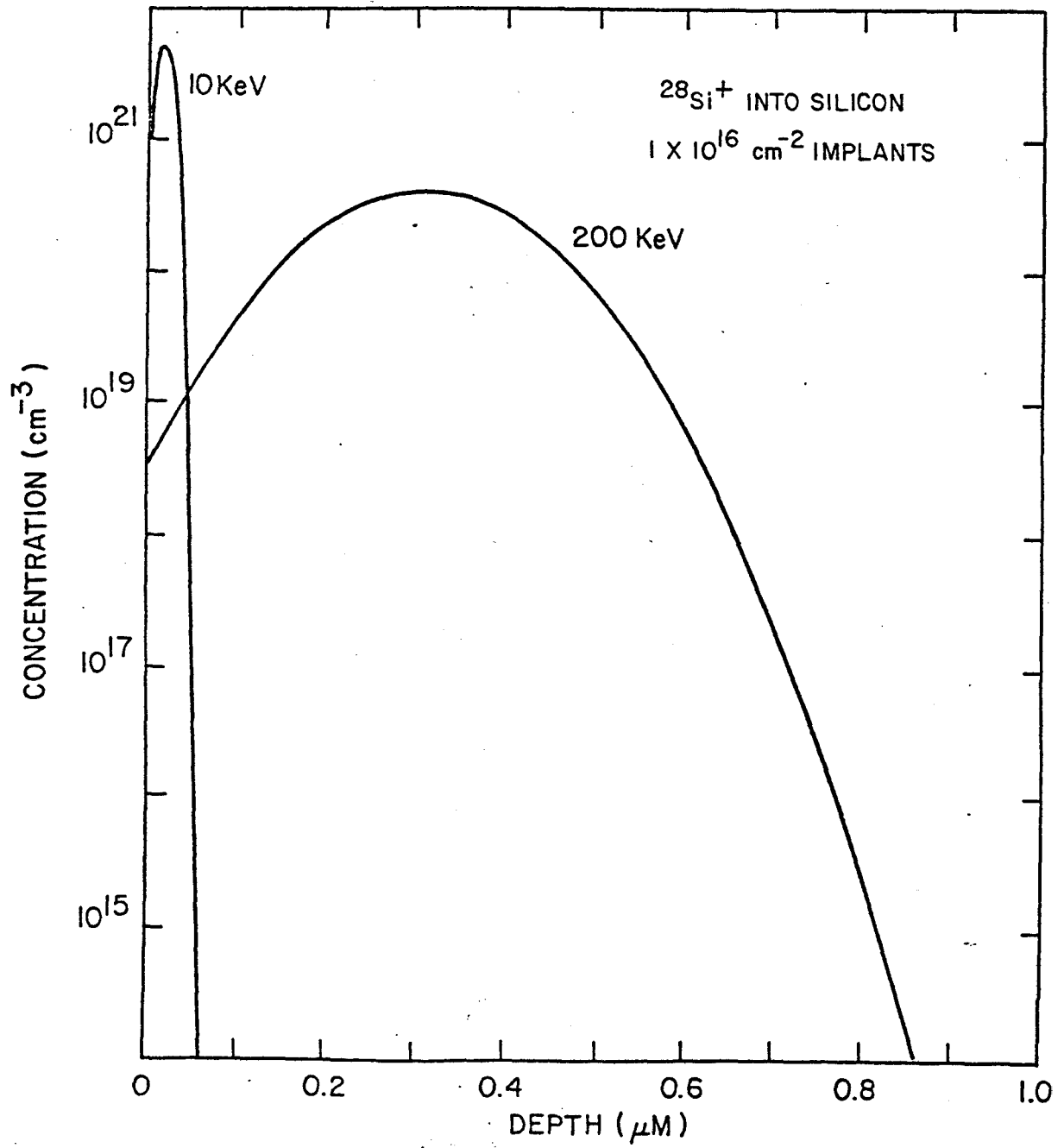


FIGURE 5. PREDICTED STOPPING DISTRIBUTIONS FOR 10 AND 200 keV $^{28}\text{Si}^+$

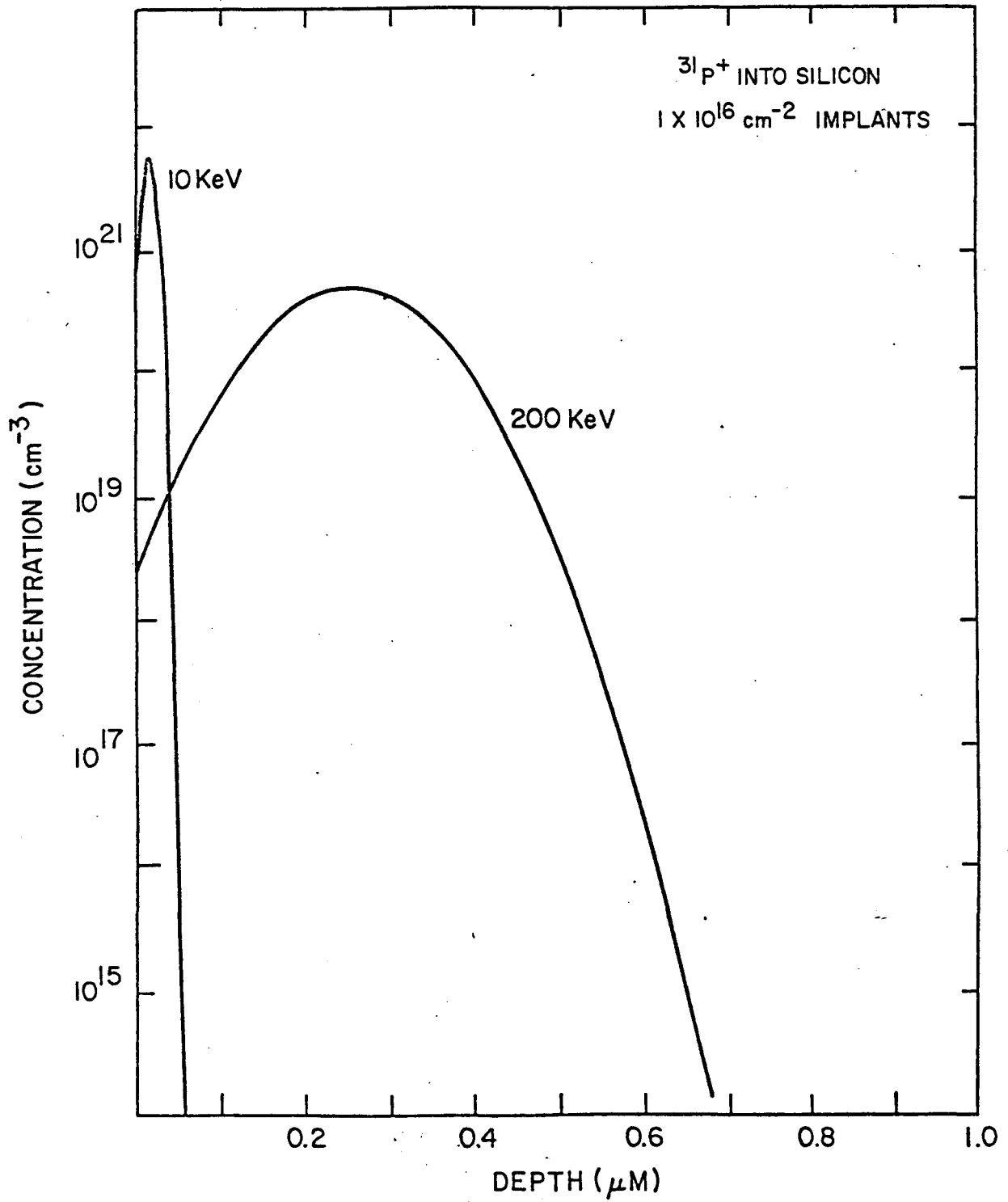


FIGURE 6. PREDICTED STOPPING DISTRIBUTIONS FOR 10 AND 200 keV $^{31}\text{P}^+$

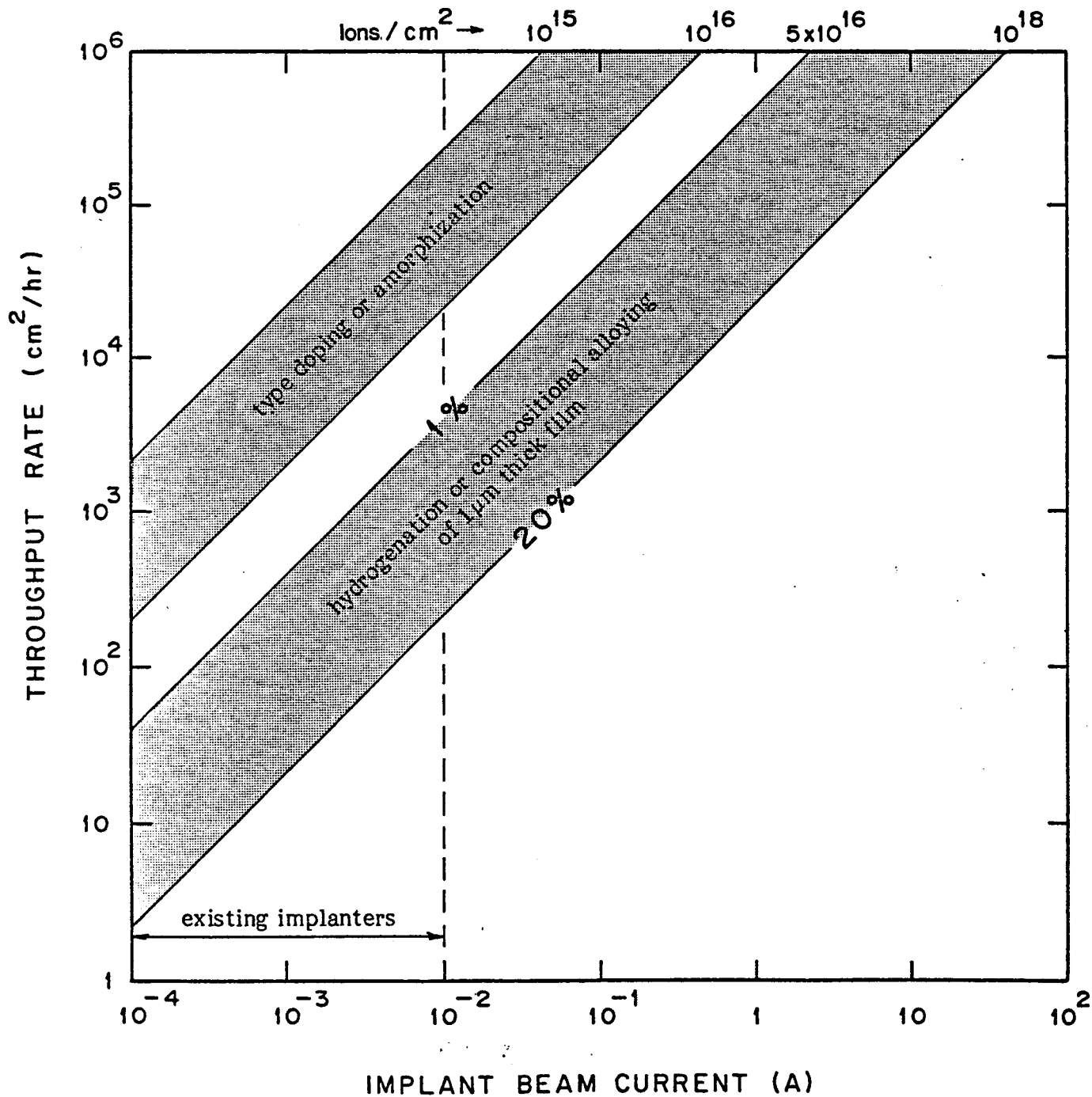


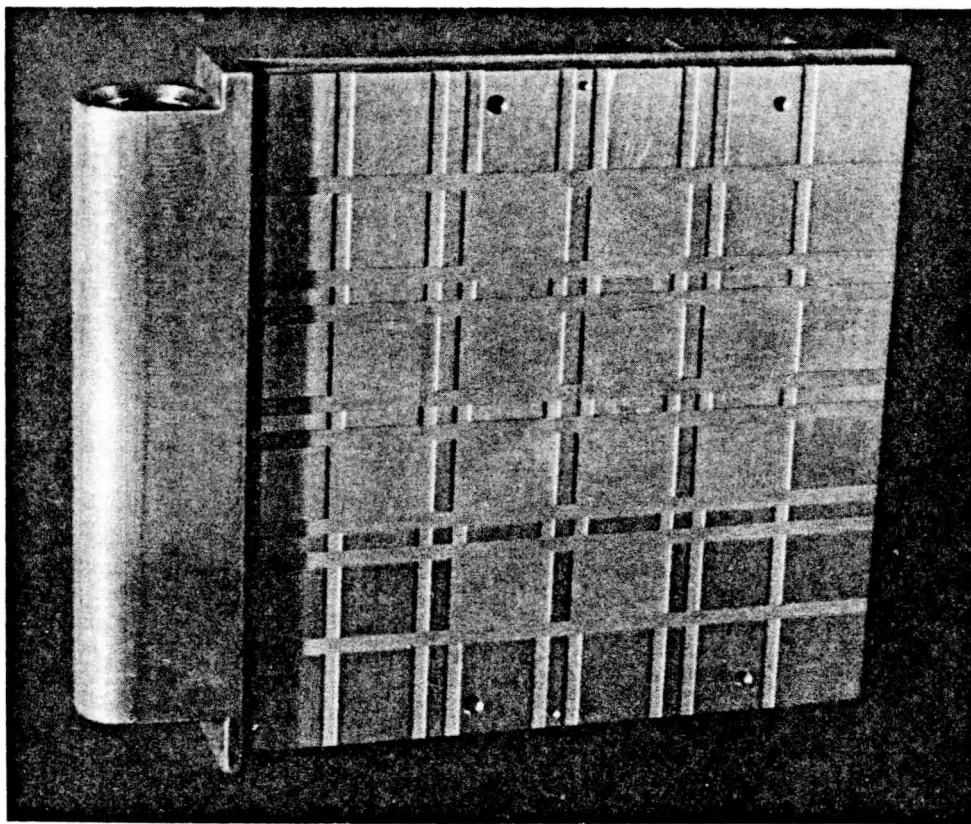
FIGURE 7. THROUGHPUT VERSUS BEAM CURRENT FOR SILICON FILM MODIFICATION PROCESSES

2.3 IMPLANTATION FACILITIES AND PROCEDURES

Two ion implanters at Spire were used for investigations under this program. Implants of $^{28}\text{Si}^+$ at energies up to 200 keV for amorphization were performed using an Extrion Model 200-20A medium current implanter. Implants of all other ions required energies of 50 keV or less and were done with a special Extrion high current solar cell implanter developed to support the JPL Low Cost Solar Array Project.

Operating conditions for the ion source of the solar cell implanter were identified which allowed at least 0.5 milliamperes of beam current of all ions of investigative interest to be delivered. A modification of the standard Freeman type source was needed to allow 0.5 milliamperes of proton beam to be produced. This modified source incorporated a hot filament within a restricted flow gas cavity fed with hydrogen gas.

The solar cell implanter used for this program was set up to deliver ion beams scanned uniformly over a region 7.6 cm in diameter on a sample holder. At 0.5 mA beam current and 50 keV ion energy, energy deposition rate into a sample surface was approximately 0.5 watt/cm^2 . During high dose implants, samples would have undergone substantial temperature elevations if some sample cooling were not provided. High substrate temperatures during implant might have caused loss of implanted hydrogen, uncontrolled partial recrystallization of the radiation damaged silicon material or possibly other effects to the disadvantage of the investigation. Consequently sample holders incorporating active cooling were designed and constructed. Figure 8 shows one such holder which was used for implanting twelve 2 x 2 cm test samples simultaneously. The holder was water cooled and samples were mounted upon it so as to provide satisfactory thermal contact. Sample temperatures during trial run implants were monitored by means of small thermocouples bonded to their surfaces. Figure 9 shows observed sample temperatures versus time for implants under different ion beam energy input conditions. With 0.5 milliamperes beam currents (maximum of 25 watts total at 50 keV) actually used for investigations under the program, sample temperatures would not rise to above 60°C .



579045P

FIGURE 8. COOLED SAMPLE HOLDER FOR SPECIAL IMPLANTATIONS

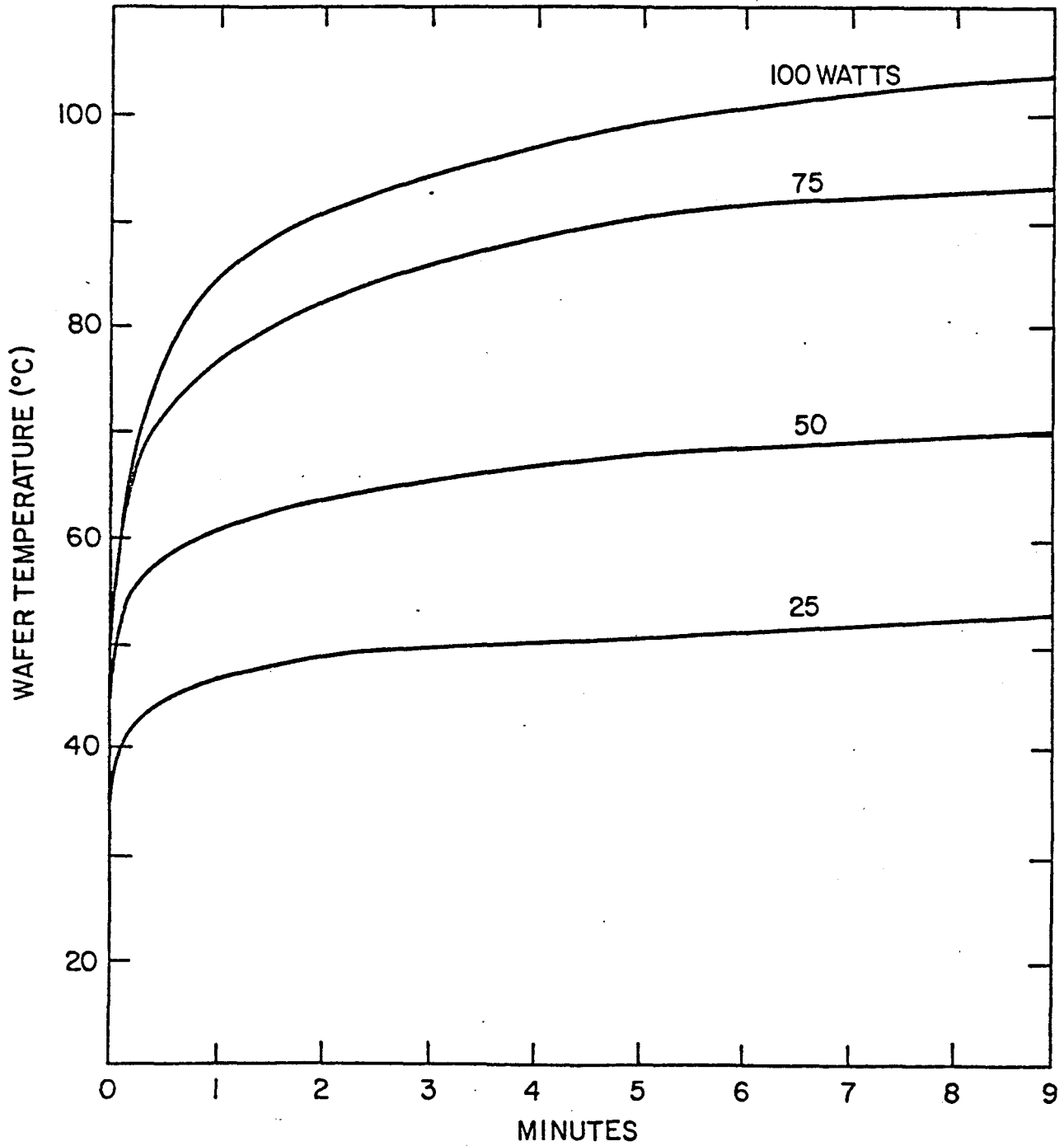


FIGURE 9. WAFER TEMPERATURE VERSUS IMPLANT TIME AS FUNCTION OF ION BEAM ENERGY INPUT

Use of the cooled sample holder in conjunction with the very high dose implants performed for the program was initially found to result in buildup of a thin film of polymerized hydrocarbons upon sample surfaces. Sample surface contamination resulting from ion beam induced polymerization of residual pump oil molecules in the vacuum chamber is a recognized implantation process effect. Generally the problem is minor because formation rates are low, implant doses are relatively small and sputtering by incoming ions tends to remove polymerized material from the surface as it is formed. However in the particular case of proton implants for hydrogenation, the doses involved are very high, 10^{17} ions/cm² or even more, and sputter removal by light $^1\text{H}^+$ ions is negligible. Early in the program it was found that polymerized hydrocarbon buildup during high dose proton implants was sufficiently severe that visible yellow films were created. During the program the problem was eliminated when for other purposes the standard oil diffusion pump for the implanter end station was replaced by a cryopump unit. Further contamination effects were not experienced.

2.4 TEST STRUCTURES

To employ ion implantation techniques to convert a nonamorphous elemental silicon host film into an amorphous silicon alloy layer with selected physical, optical and electrical characteristics represents a significant extension of the range of applications for which implantation has been generally considered. In-depth investigation of all the process phenomena and mechanisms which could be encountered is far beyond the scope of the overview study which could be conducted under this program. The purpose of the planned program was to survey the identified prospective applications of implantation to determine their feasibility and merit and then to attempt to empirically identify process conditions which could be employed to fabricate operational amorphous silicon solar cells. In this type of program it is easy to change implantation process parameters but much more difficult to assess the effect or value of the changes. Methods to evaluate particular implantation effects on properties of interest in fabricating an amorphous silicon cell were needed. Two primary test structures were selected — a material test sample and a solar cell test device sample.

The material test structure consisted simply of a nominally 0.5 micrometer thick silicon film deposited by chemical vapor deposition onto a 2 x 2 cm slide of type 7940 fused silica. Another structure in which the silicon film was deposited onto an oxidized silicon wafer was also used for electrical conductivity evaluations but was found to yield erroneous results. As-deposited silicon films were intended to be undoped and were polycrystalline with average grain diameters 0.1 micrometer or less. The silicon film on fused silica slide material test structure samples were used to directly examine the effect of given implantation conditions upon the electrical conductivity and optical transmittance of the implanted silicon. Because the silicon films on the fused silica slides were only 0.5 micrometer thick, implantation conditions employed were generally such that approximately uniform effects through the film would be expected.

In order to obtain initial information regarding the effects of the various implantation process upon possible operational behavior of amorphous silicon cells, a solar cell device test structure was utilized. Configuration of the device test structure is shown in Figure 10. These device structures were fabricated from vapor deposited boron-doped polycrystalline films on thermally oxidized silicon wafers. Each 2 x 2 cm test unit consisted of nine individual n^+/p implanted junction cells of area 0.1 cm^2 which were initially operational as polycrystalline silicon film devices. It was intended that the effects of amorphization by $^{28}\text{Si}^+$ implantations, of hydrogenation by $^1\text{H}^+$ implantation and of various thermal or electron beam annealing procedures on device operation could be observed by measuring illuminated I-V characteristics and spectral response characteristics of the test cells. Figure 11 shows initial as-fabricated AM0 I-V characteristics of the nine cell devices on a test unit. Small grain structure of the thin polysilicon films and high series resistance values resulting from the inadequate method of making back contact were responsible for limitations upon performance of the cell devices. It was not intended that the test devices would represent good cells but rather that they were to be used to examine changes in operational behavior which could be caused by various prospective implantation processes.

2.5 IMPLANTATION EFFECTS INVESTIGATION

2.5.1 Material Modifications Studies

Material studies which were performed involved examination of $^1\text{H}^+$ and $^{28}\text{Si}^+$ implants in conjunction with low temperature thermal annealing or low dose pulsed electron beam annealing. Most investigations employed 0.5 micrometer thick undoped CVD polycrystalline silicon films on fused silica slides as previously described.

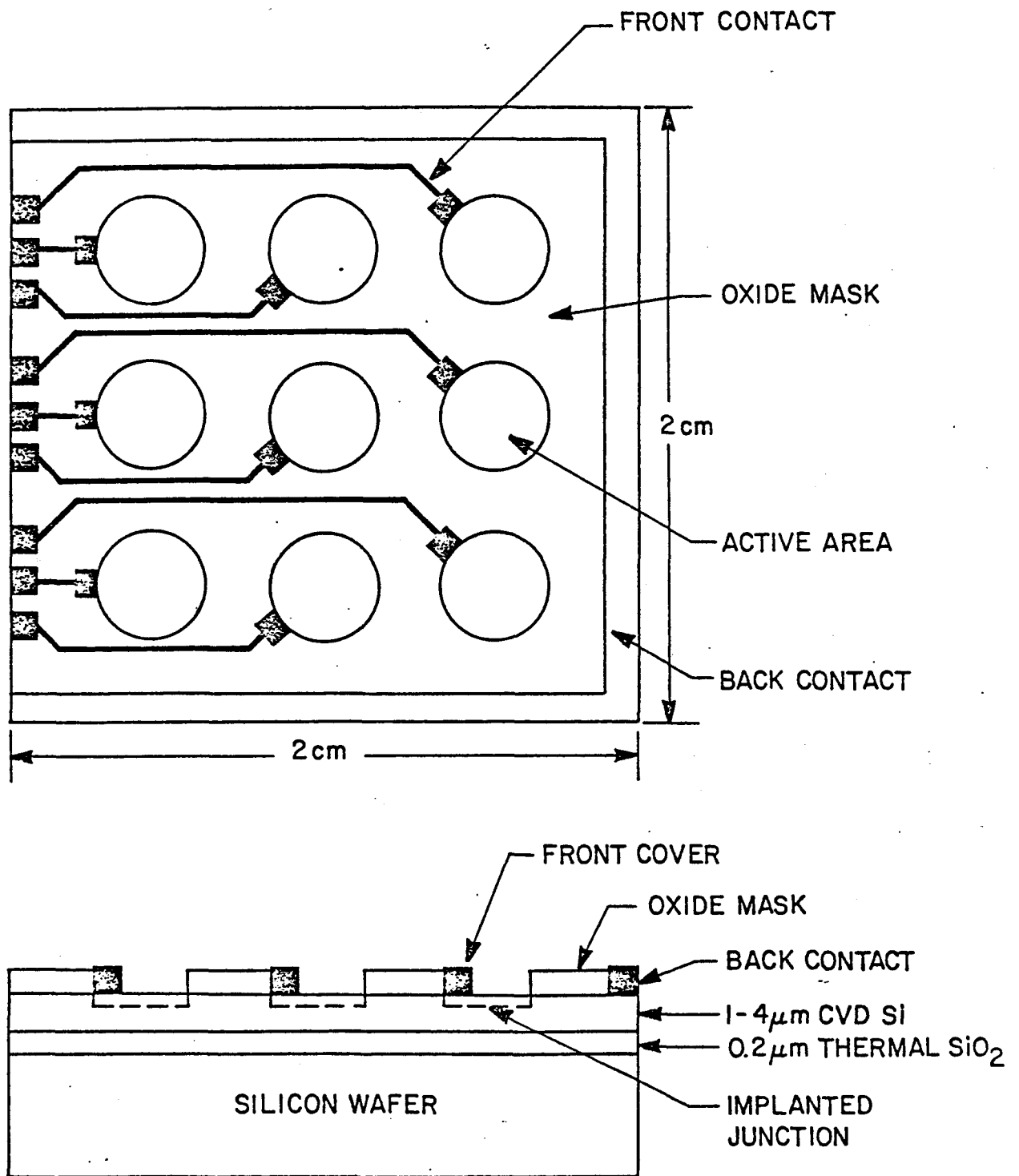


FIGURE 10. CELL DEVICE TEST STRUCTURE

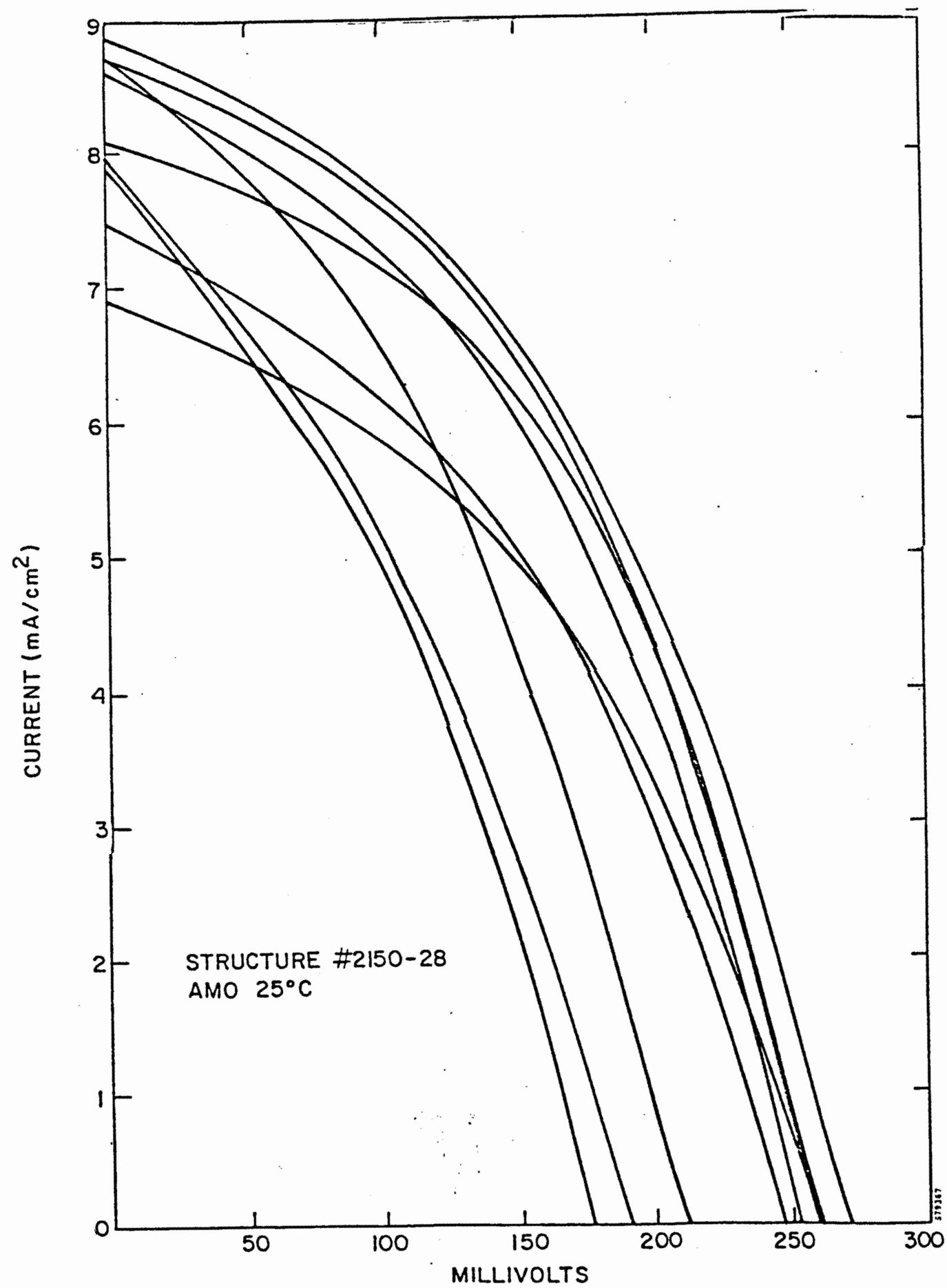


FIGURE 11. ILLUMINATED OUTPUT CHARACTERISTICS OF NINE POLYSILICON CELL DEVICES ON TEST STRUCTURE

A penetrating ion produces structural damage to a material as it undergoes collisional stopping. Heavy ions can destroy the crystallinity of a silicon layer into which they are implanted but because the proton is light, $^1\text{H}^+$ implantation causes only minor damage to the silicon lattice. The relationships of the properties of amorphous silicon layers produced by using ion implantation to eliminate crystallinity to the properties which are to be necessary for an amorphous silicon solar cell have not yet been fully identified. For the program which has been conducted it was desired that implantation conditions to be used for amorphization purposes be very carefully selected to insure total removal of identifiable crystallinity within the silicon layer. Helium ion backscattering studies have shown that crystalline order can be eliminated to a depth of approximately 0.5 micrometer by using a set of four $^{28}\text{Si}^+$ implants performed with diffuse ion beams into silicon held at liquid nitrogen temperature:

| | |
|---------|---|
| 200 keV | 3×10^{15} ions/cm ² |
| 150 keV | 2×10^{15} ions/cm ² |
| 100 keV | 2×10^{15} ions/cm ² |
| 50 keV | 1×10^{15} ions/cm ² |

Stopping distribution for this set of implants are shown in Figure 12. Although less stringent conditions might be usable in future work, implants for amorphization purposes under this program were usually performed using these parameters.

Figure 13 shows optical transmittance versus wavelength measurements from a fused silica slide with 0.5 micrometer thick silicon film (i) after deposition of the polycrystalline film by CVD, (ii) after $^{28}\text{Si}^+$ implantation to amorphize the silicon and (iii) after low temperature thermal annealing intended to restore short range order within the amorphous silicon. To the eye, the effect of the amorphizing $^{28}\text{Si}^+$ implants was to transform the translucent red-brown 0.5 micrometer thick silicon film into a reflective opaque grey layer. It can be seen from Figure 13 that $^{28}\text{Si}^+$ implantation caused optical absorption coefficient of the implant-damaged silicon to be increased to at least 10^5 cm⁻¹ for all wavelengths less than 600nm.

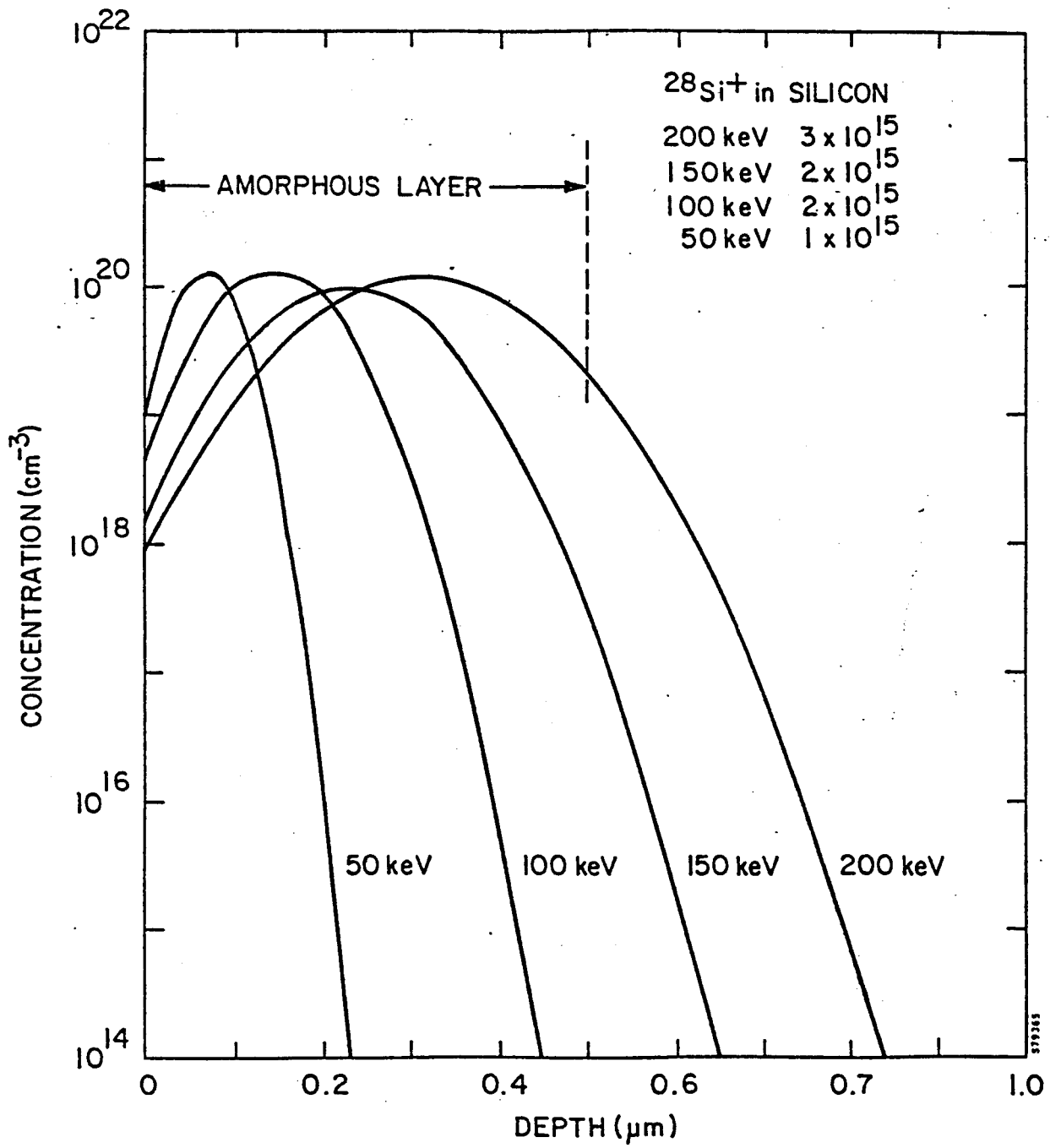


FIGURE 12. $^{28}\text{Si}^+$ IMPLANTS USED FOR AMORPHIZATION OF POLYSILICON FILM

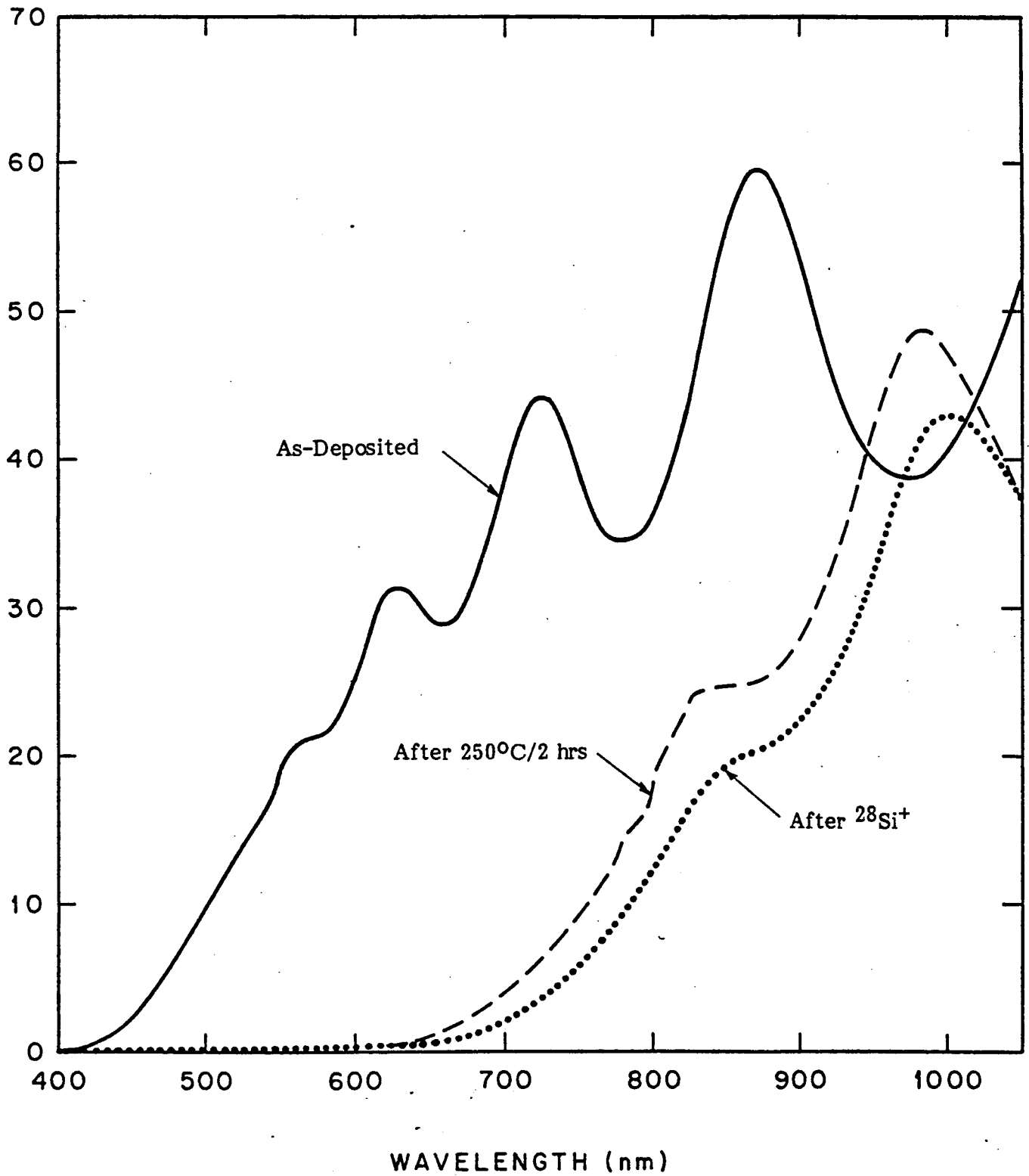


FIGURE 13. TRANSMITTANCE VERSUS WAVELENGTH OF 0.5 μm SILICON FILM AMORPHIZED BY $^{28}\text{Si}^+$ IMPLANT

Distribution of hydrogen implanted into silicon at only a single energy is very nonuniform. In order to distribute implanted hydrogen over a layer of thickness comparable to the depth which could be amorphized by $^{28}\text{Si}^+$ implantation, a set of three $^1\text{H}^+$ ion energies, 12, 20 and 30 keV, was normally used for hydrogen introduction. Example individual and composite stopping distribution profiles are shown in Figure 14. The same relative doses at each energy level were maintained for all total dose levels utilized.

Figures 15, 16 and 17 present optical transmittance versus wavelength data from films exposed to total $^1\text{H}^+$ doses of 3×10^{16} , 1×10^{17} and 3×10^{17} ions/cm², respectively. It can be seen that the hydrogen implantation did cause minor reduction of transmittance and that the effect upon transmittance of $^1\text{H}^+$ implantation increases with increasing dose but in all cases was much less than that caused by $^{28}\text{Si}^+$ implantation as was shown in Figure 13. Hydrogen implantation did not cause the major increases in film absorption below 650 nm which were observed with amorphous implants of $^{28}\text{Si}^+$. It is also to be noted that annealing at 250°C in nitrogen after $^1\text{H}^+$ implantation caused no appreciable change in transmittance characteristics of the films.

Figure 18 shows optical transmittance versus wavelength data from a film which was first implanted with $^1\text{H}^+$ to a dose of 3×10^{16} ions/cm² then amorphized by $^{28}\text{Si}^+$ implantation and finally annealed at 250°C for 2 hours in nitrogen. Figure 19 shows data from a sample processed similarly except that the hydrogen implant dose was 3×10^{17} ions/cm². The effect upon optical transmittance of a $^{28}\text{Si}^+$ amorphizing implant when hydrogen is present in the silicon film seems essentially the same as when hydrogen is not present except that relatively high hydrogen content, the 3×10^{17} ions/cm² dose case of Figure 19, may have reduced absorption behavior at the cut-on edge, i.e., between 600 and 650 nm.

In addition to transmittance measurements in the spectral range 400 to 1100 nm made on silicon films deposited upon fused silica slide substrates, a few IR transmittance measurements were made early in the program on films used in cell device test structures which were described in Section 2.4. Samples in this case consisted of approximately 3 micrometers of CVD polycrystalline silicon over 0.2 micrometer of grown oxide on a single crystal silicon wafer. Implants of $^1\text{H}^+$ or $^{28}\text{Si}^+$ were made into the surface of the polycrystalline silicon layer. Figure 20 shows two example IR transmittance plots, the first from a sample implanted with 3×10^{17} $^1\text{H}^+$ ions/cm² at 50 keV and the second from a sample implanted first with $^{28}\text{Si}^+$ for amorphization, then

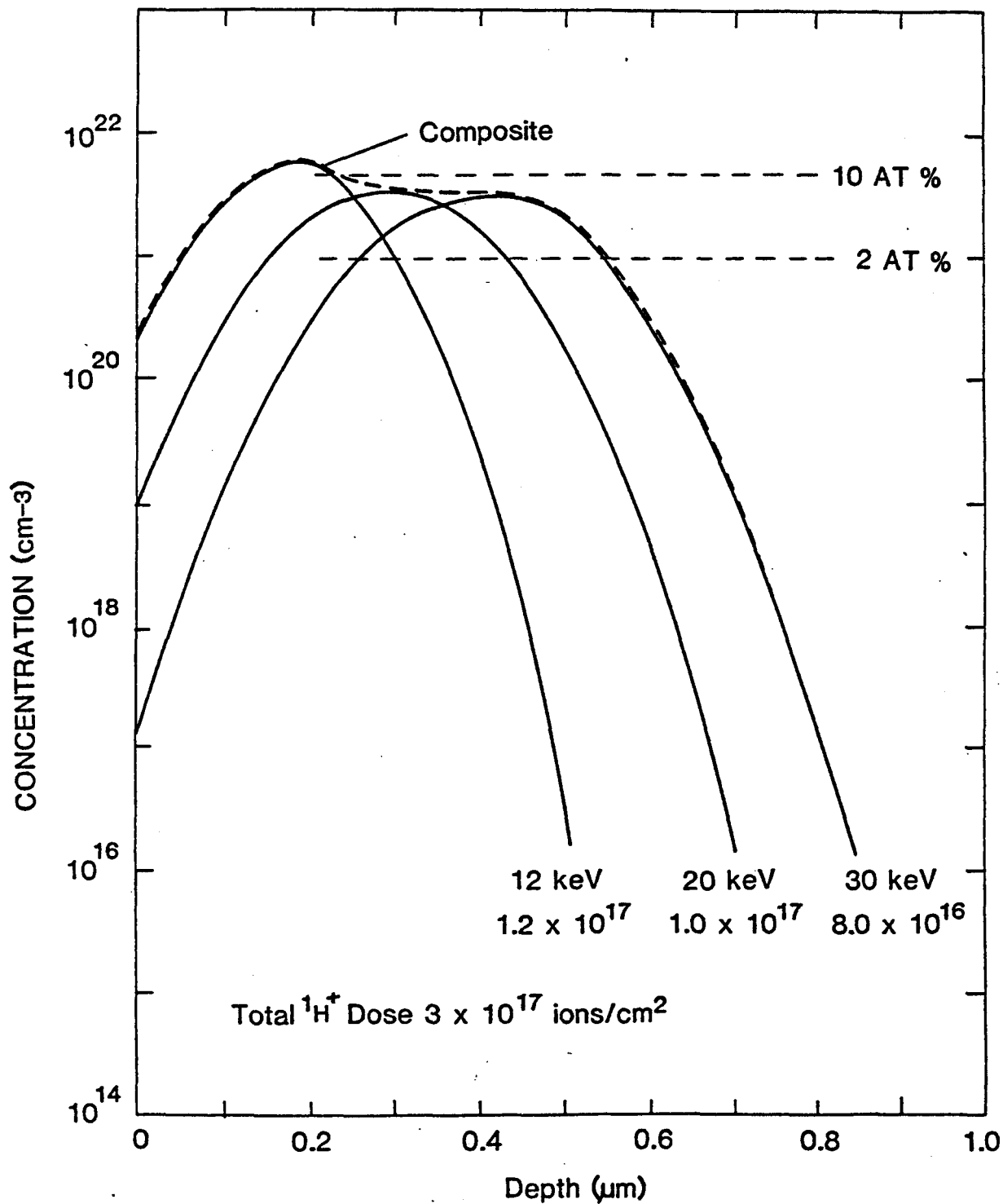


FIGURE 14. PREDICTED DISTRIBUTION OF HYDROGEN IN SILICON FROM COMBINED 12, 20 AND 30 keV ¹H⁺ IMPLANTS

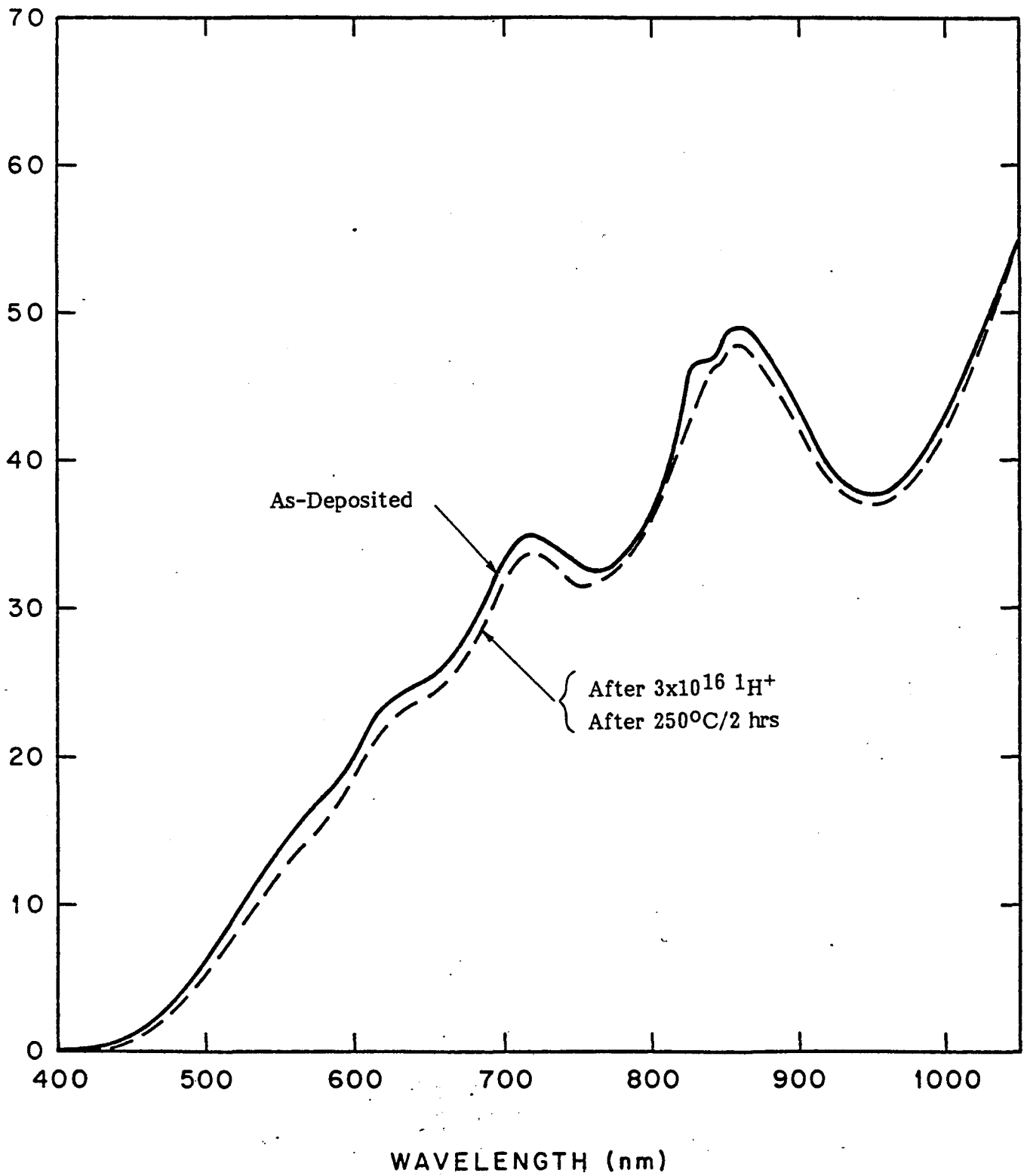


FIGURE 15. TRANSMITTANCE VERSUS WAVELENGTH OF 0.5 μm SILICON FILM IMPLANTED WITH 3×10^{16} 1H^+ IONS/ CM^2

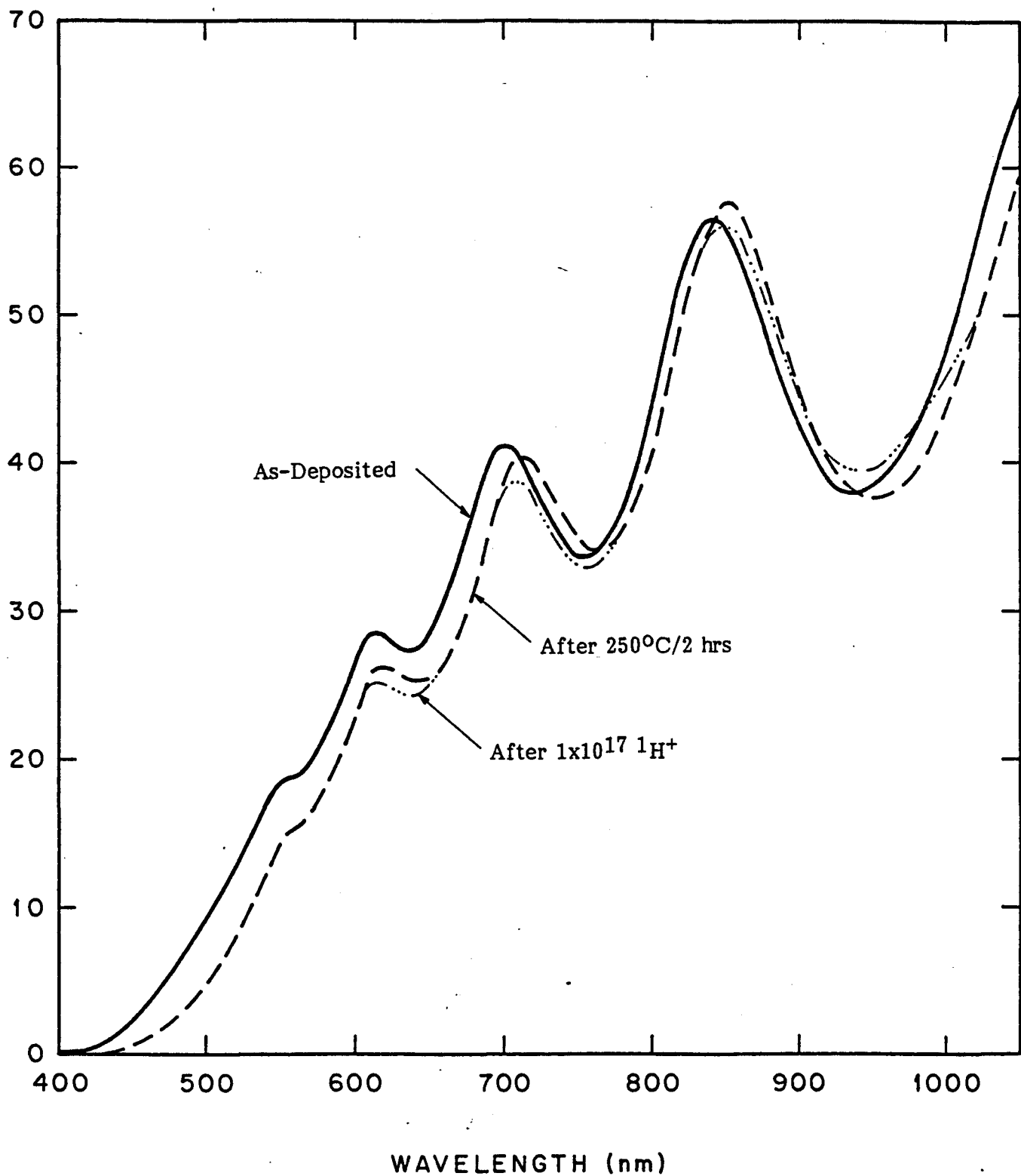


FIGURE 16. TRANSMITTANCE VERSUS WAVELENGTH OF 0.5 μm SILICON FILM IMPLANTED WITH 1×10^{17} 1H^+ IONS/ CM^2

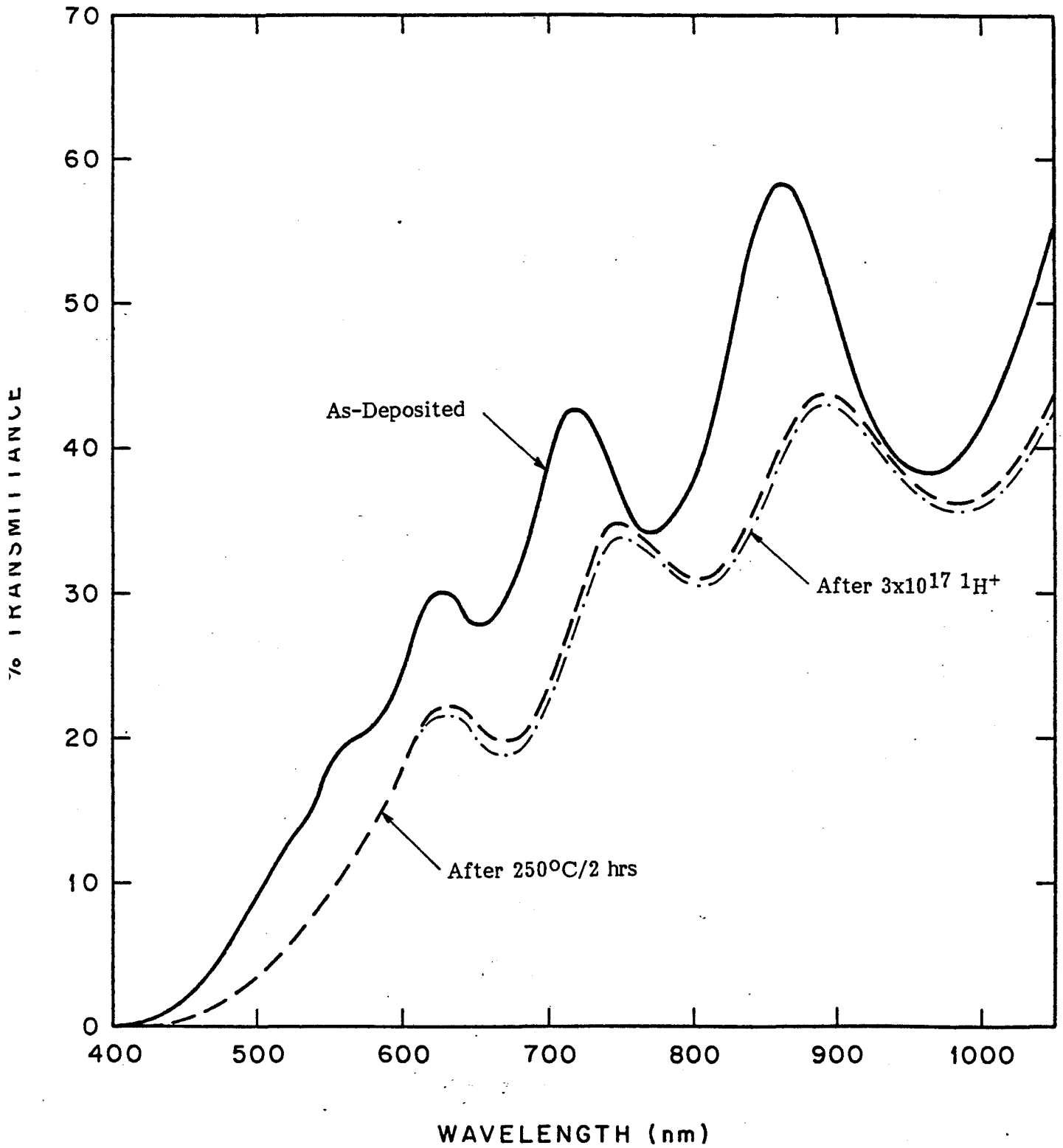


FIGURE 17. TRANSMITTANCE VERSUS WAVELENGTH OF 0.5 μm SILICON FILM IMPLANTED WITH 3x10¹⁷ 1H⁺ IONS/CM²

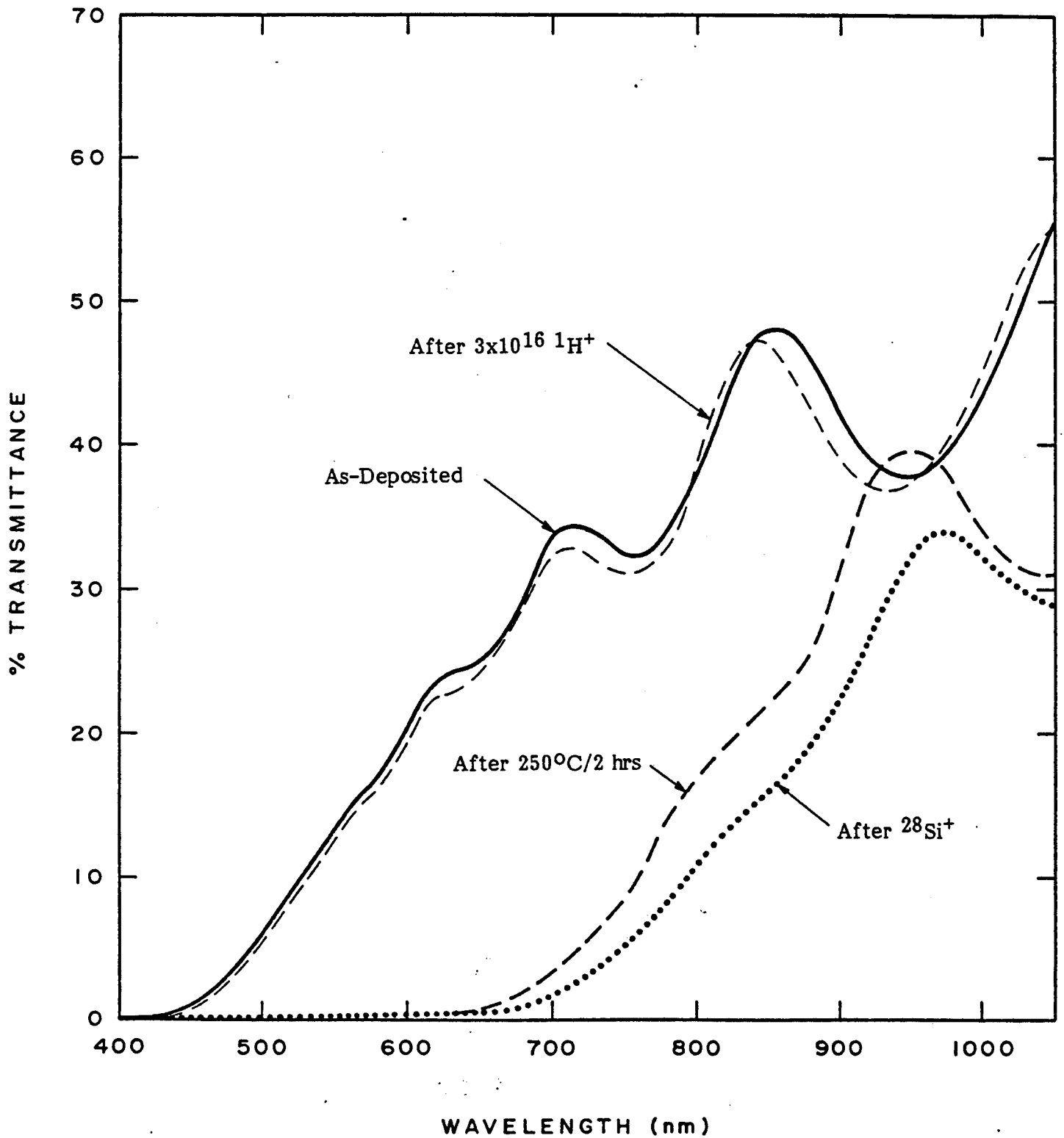


FIGURE 18. TRANSMITTANCE VERSUS WAVELENGTH OF 0.5 μm SILICON FILM IMPLANTED WITH 3×10^{16} $^1\text{H}^+$ IONS/ CM^2 AND AMORPHIZED BY $^{28}\text{Si}^+$ IMPLANTS

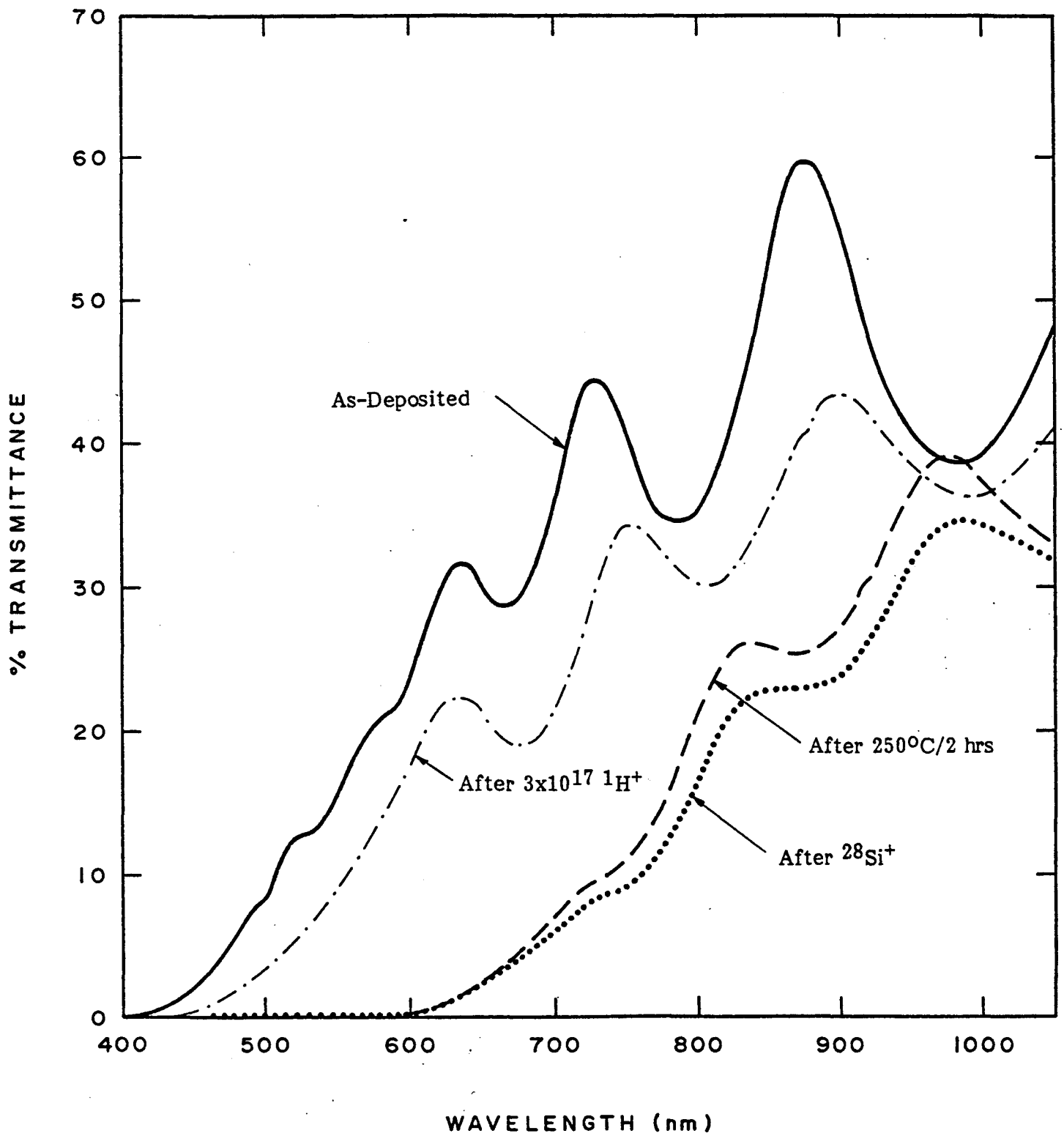


FIGURE 19. TRANSMITTANCE VERSUS WAVELENGTH OF $0.5 \mu\text{m}$ SILICON FILM IMPLANTED WITH $3 \times 10^{17} \text{ } ^1\text{H}^+$ IONS/ CM^2 AND AMORPHIZED BY $^{28}\text{Si}^+$ IMPLANT

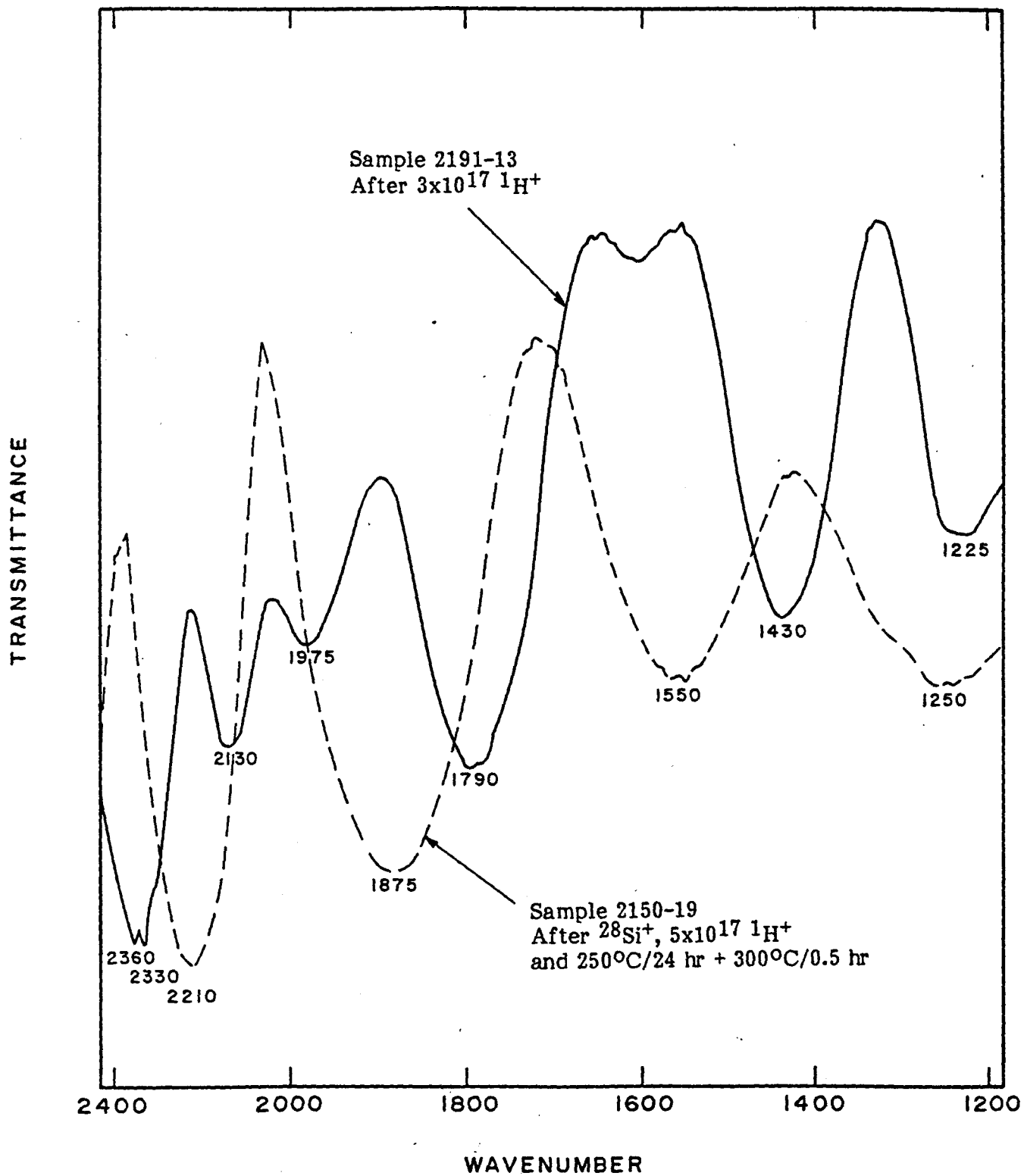


FIGURE 20. RELATIVE INFRARED TRANSMITTANCE VERSUS WAVENUMBER FROM SILICON FILMS ON SILICON WAFER SUBSTRATES

with $3 \times 10^{17} \text{ } ^1\text{H}^+$ ions/cm² at 50 keV and $1 \times 10^{17} \text{ } ^1\text{H}^+$ ions/cm² at 10 keV, followed by annealing for several hours at temperatures up to 300°C. Distinct differences between the two spectra are evident. Use of IR measurements could not be pursued under this program, but it is believed that IR transmittance measurements correlated with other data would represent a particularly useful method to monitor a series of methodical variations of implantation parameters used to prepare or to modify amorphous silicon layers.

It is evident that, while ignoring questions regarding microscale physics, ion implantation can be utilized to modify crystallinity of a silicon film, to change its optical absorption characteristics and to controllably introduce hydrogen to the location desired. In simplest terms the merit of any material to be incorporated into a photovoltaic device is determined by the optical characteristics and the electrical properties of that material. In conjunction with evaluations of variations produced in optical absorption behavior of silicon films, the effects of implantation processes upon dark conductivity and photoconductivity were to be examined.

A matrix of implantation processes and annealing tests was conducted upon a set of samples intended for determination of electrical characteristics. The samples were 2x2 cm pieces of single crystal silicon wafer with approximately 0.2 micrometer of thermally grown SiO₂ upon which had been deposited by CVD 0.5 micrometer of undoped polycrystalline silicon as the test material. This type of sample was easily fabricated and handled, was thermally stable to even very high furnace temperatures and could be subjected to pulsed electron beams for transient annealing test purposes. A considerable amount of information regarding dark conductivity and photoconductivity versus implantation and annealing process conditions was compiled using these samples. Unfortunately the data obtained was found to be not reproducible. It was determined that, as a result of handling during processing and testing, minor abrasion of the sample surfaces could cause loss of local integrity of the SiO₂ film which isolated the silicon layer of interest from its silicon wafer substrate. Since effective resistances of the initially undoped polycrystalline test films could be much higher than resistance values of spurious shunt paths involving the substrate, erroneous measurements were able to result. Because it is not possible to separate with certainty the valid and erroneous data, results from these samples have not been utilized.

In the absence of reliable information from planned conductance evaluations, conductivity measurements were made upon the 0.5 micrometer thick silicon films on fused silica slide samples used for optical transmittance evaluations described above. The number of process parameter variations for which these samples were available was somewhat limited, but the general effects of $^1\text{H}^+$ and $^{28}\text{Si}^+$ implant upon the initially undoped films are evident. Conductivity values from these samples are given in Table I. It can be observed that:

- (i) Implantation of hydrogen not followed by annealing did not significantly change dark conductivity of the films but substantially reduced photoconductivity, probably to a greater extent with increasing dose.
- (ii) A short 2 hour anneal at 250°C did not appreciably alter conductivities of films implanted only with hydrogen. Longer 20 hour anneals at 250°C caused several orders of magnitude increase in conductivity values with the smallest increases occurring at highest dose.
- (iii) An amorphizing silicon implant followed by short anneal caused more than two orders of magnitude increase in dark conductivity but longer annealing reduced conductivity.
- (iv) The presence of implanted hydrogen in the films prior to the amorphizing silicon implant and low temperature furnace anneal decreased the effect of the amorphization upon dark conductivity and caused photoconductivity to be reduced to below as-deposited film values; the degree of reduction was very dependent upon hydrogen dose and annealing conditions.

It is important to recognize that these results regarding effects of hydrogen and silicon ion implantation upon conductivity apply to the case of silicon films which were undoped. The effects of the presence of dopants or of varied annealing procedures were not examined. The results in Table I indicate that methods to allow controlled selection of conductivity characteristics must be investigated.

TABLE I. CONDUCTIVITY VALUES OF 0.5 μ m CVD SILICON FILMS ON FUSED SILICA SLIDES

| | Conductivity 10 ⁻⁶ (ohm-cm) ⁻¹ | |
|--|---|-------------|
| | Dark | Illuminated |
| <u>Unimplanted Films</u> | | |
| #1 As-deposited | 0.24 | 37 |
| #2 As-deposited | 0.58 | 29 |
| #2 After 250°C/20 hr | 0.48 | 36 |
| #3 As-deposited | 0.62 | 40 |
| #3 After 250°C/20 hr | 0.48 | 40 |
| #4 As-deposited | 0.31 | 27 |
| <u>Films Implanted with Hydrogen</u> | | |
| 3 x 10 ¹⁶ ¹ H ⁺ | 0.76 | 4.0 |
| 3 x 10 ¹⁶ ¹ H ⁺ then 250°C/2 hr | 1.0 | 3.1 |
| 3 x 10 ¹⁶ ¹ H ⁺ then 250°C/20 hr | 30,000 | 38,000 |
| 1 x 10 ¹⁷ ¹ H ⁺ | 0.36 | 2.0 |
| 1 x 10 ¹⁷ ¹ H ⁺ then 250°C/2 hr | 0.64 | 3.1 |
| 1 x 10 ¹⁷ ¹ H ⁺ 250°C/20 hr | 1,400 | 3,400 |
| 3 x 10 ¹⁷ ¹ H ⁺ | 0.53 | 1.4 |
| 3 x 10 ¹⁷ ¹ H ⁺ then 250°C/2 hr | 0.47 | 1.8 |
| 3 x 10 ¹⁷ ¹ H ⁺ then 250°C/20 hr | 7.1 | 270 |
| <u>Films Amorphized by Silicon Implantation</u> | | |
| ²⁸ Si ⁺ then 250°C/2 hr | 110 | 140 |
| ²⁸ Si ⁺ then 250°C/20 hr | 5.6 | 6.2 |
| 3 x 10 ¹⁶ ¹ H ⁺ then ²⁸ Si ⁺ then 250°C/2 hr | 8.0 | 10 |
| 3 x 10 ¹⁶ ¹ H ⁺ then ²⁸ Si ⁺ then 250°C/20 hr | 0.01 | 0.14 |
| 3 x 10 ¹⁷ ¹ H ⁺ then ²⁸ Si ⁺ then 250°C/2 hr | 0.42 | 0.62 |
| 3 x 10 ¹⁷ ¹ H ⁺ then ²⁸ Si ⁺ then 250°C/20 hr | 0.63 | 3.1 |

2.5.2 Device Characteristics Studies

The test device structure which was described in Section 2.4 and shown in Figure 10 was used to examine the effects of $^1\text{H}^+$ or/and $^{28}\text{Si}^+$ implantation upon operational performance of small crude solar cells which started as n^+/p implanted junction polycrystalline silicon film devices. Generally the observed effects upon performance of these units correlate with effects described above on material test samples.

In the case of $^1\text{H}^+$ implants made into functional polycrystalline film devices, the effect upon performance was always to degrade short circuit current density and open circuit voltage of the device. Degree of performance degradation increased with increasing hydrogen ion dose. A minor amount of the lost performance could be restored by means of a low temperature thermal anneal or low dose electron beam pulse anneal. Figure 21 shows AM0 current-voltage characteristics from a typical 0.1 cm^2 cell device on a nine device test sample which was exposed to a $^1\text{H}^+$ dose of 1×10^{17} ions/ cm^2 . The observed performance loss can probably be attributed to reduction of carrier lifetime in the polycrystalline silicon forming the cell.

When polysilicon device test samples were implanted with $^{28}\text{Si}^+$ to cause amorphization of the first 0.5 micrometer of the approximately 3 micrometer thick polycrystalline film comprising the cell structure, major loss of device performance was observed. Low temperature thermal annealing or electron beam pulse annealing would not cause performance restoration and in fact would usually result in additional output reduction. Figure 22 shows AM0 current-voltage characteristics from a typical individual cell on a test sample. The loss of performance is believed to be a result of the severe degradation of carrier lifetime associated with the silicon ion implantation damage.

Device samples implanted with $^1\text{H}^+$ for hydrogenation and with $^{28}\text{Si}^+$ for amorphization exhibited different forms of performance behavior. Output losses were still large but of changed character. Figure 23 shows AM0 current-voltage characteristics of one device on a test sample subjected first to 3×10^{17} $^1\text{H}^+$ ions/ cm^2 , then to $^{28}\text{Si}^+$ for amorphization, then to an additional 2×10^{17} $^1\text{H}^+$ ions/ cm^2 and finally to anneal cycles of 24 hours at 250°C and then 30 minutes at 300°C . It can be seen that

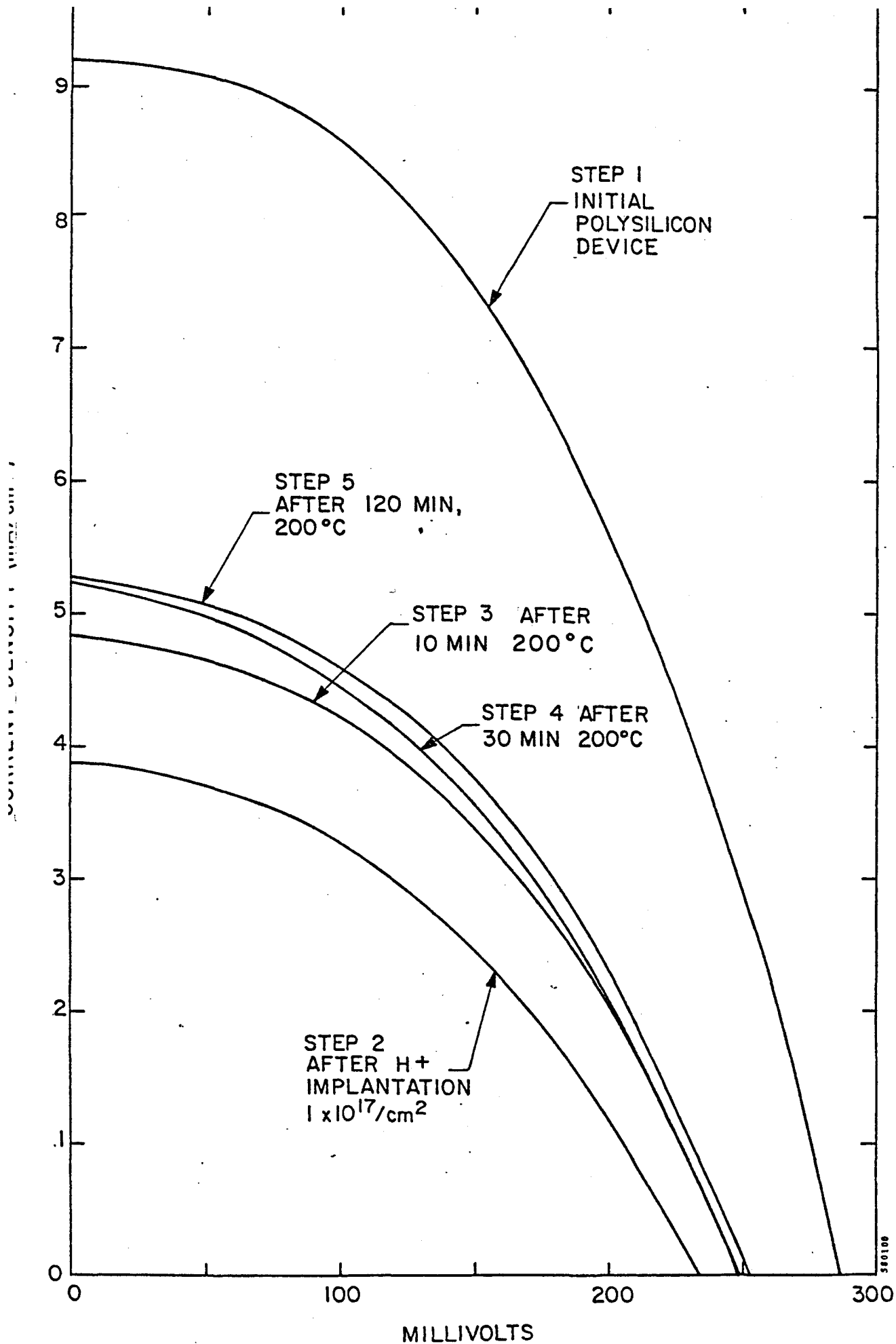


FIGURE 21. AM0 CURRENT DENSITY VERSUS VOLTAGE OF 0.1 cm² DEVICE IMPLANTED WITH 1x10¹⁷ H⁺ ions/cm²

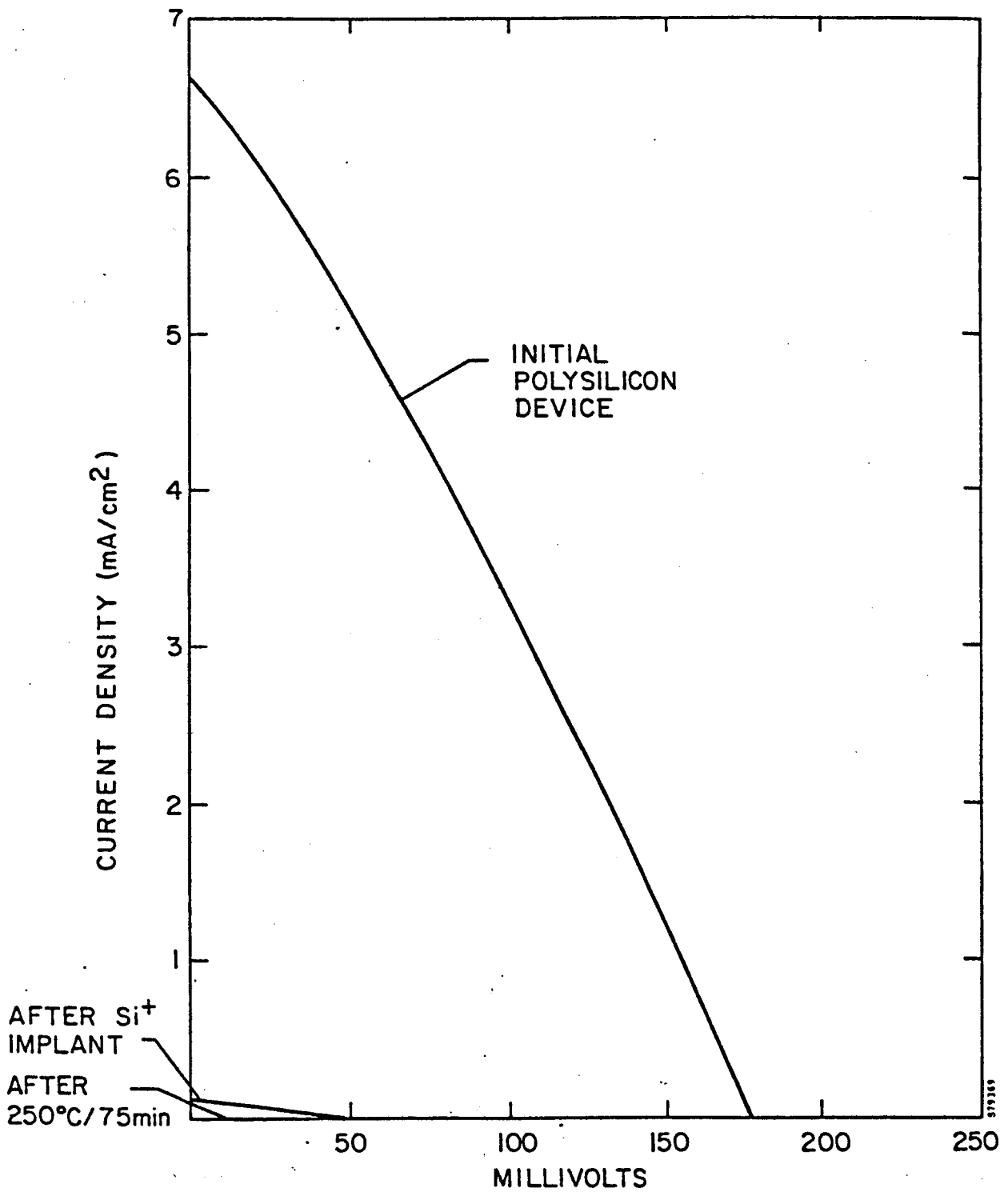


FIGURE 22. AM0 CURRENT DENSITY VERSUS VOLTAGE OF 0.1 cm² DEVICE WITH AMORPHIZING ²⁸Si⁺ IMPLANT

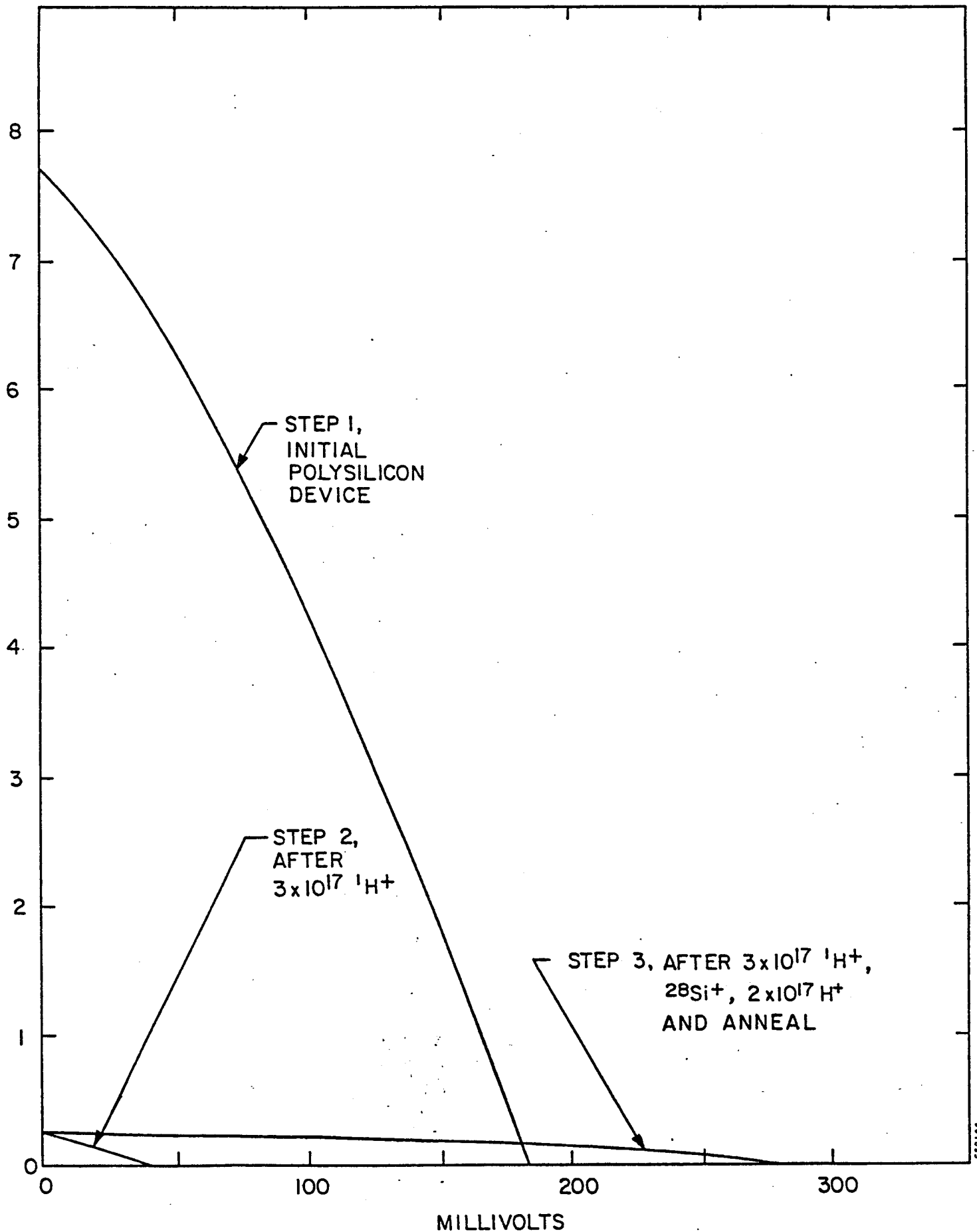


FIGURE 23. AM0 CURRENT DENSITY VERSUS VOLTAGE CHARACTERISTICS OF 0.1 cm^2 DEVICE WITH $^1\text{H}^+$ AND $^{28}\text{Si}^+$ IMPLANTS

while short circuit current density of the device decreased from 7.7 mA/cm^2 to 0.3 mA/cm^2 , open circuit voltage rose from 180 mV to 270 mV. When such devices were operated under multiple sun illumination, short circuit current increased linearly with intensity and open circuit voltage increased as $\ln(J_{sc})$.

It is believed that the polysilicon cell devices implanted with $^1\text{H}^+$ and $^{28}\text{Si}^+$ to perform as indicated above were converted into amorphous film cells of very ineffective structure. The devices had 0.3 micrometer deep n^+/p junctions. Amorphization by $^{28}\text{Si}^+$ implantation caused photon absorption to shift to the region close to the surface which was heavily phosphorus doped. Inability to collect generated carriers in such a configuration might explain the low current densities, whereas amorphous material character could be responsible for relatively very high open circuit voltages.

2.6 AMORPHOUS CELL EXPERIMENT

As this program neared completion an attempt was made to fabricate a $2 \times 2 \text{ cm}$ amorphous silicon cell. Investigations under this program had been conducted on initially polycrystalline silicon films deposited by CVD, and Spire did not have apparatus which could deposit amorphous silicon films directly. Consequently it was necessary to use CVD for deposition of films to be used in a $2 \times 2 \text{ cm}$ experimental cell. This presented serious difficulties, particularly in selecting a usable substrate and making an acceptable back contact to the deposited silicon film. For lack of a better approach, it was decided that CVD films would be deposited onto pieces of graphite sheet which would have to serve as back contacts and from which impurities of unknown type and concentration would certainly migrate into the silicon during film deposition. Initially 5 micrometers of CVD p^+ film heavily doped with boron were deposited, and then 1 micrometer of film without intentional doping was added. A shallow n^+ junction layer was introduced using 5 keV phosphorus ion implantation and furnace annealing at 750°C for 30 minutes. Implants of $^1\text{H}^+$ and/or $^{28}\text{Si}^+$ were then performed and a simple front contact grid was evaporated onto the film surface. The resulting structure was that suggested in Figure 24. The set of cells fabricated included a cell without $^1\text{H}^+$ or $^{28}\text{Si}^+$ implants, cells with $^1\text{H}^+$ implants alone at dose levels 3×10^{16} , 1×10^{17} or 3×10^{17} ions/cm² and cells with these $^1\text{H}^+$ implants followed by $^{28}\text{Si}^+$ implants. Anneals were 250°C for 2 hours.

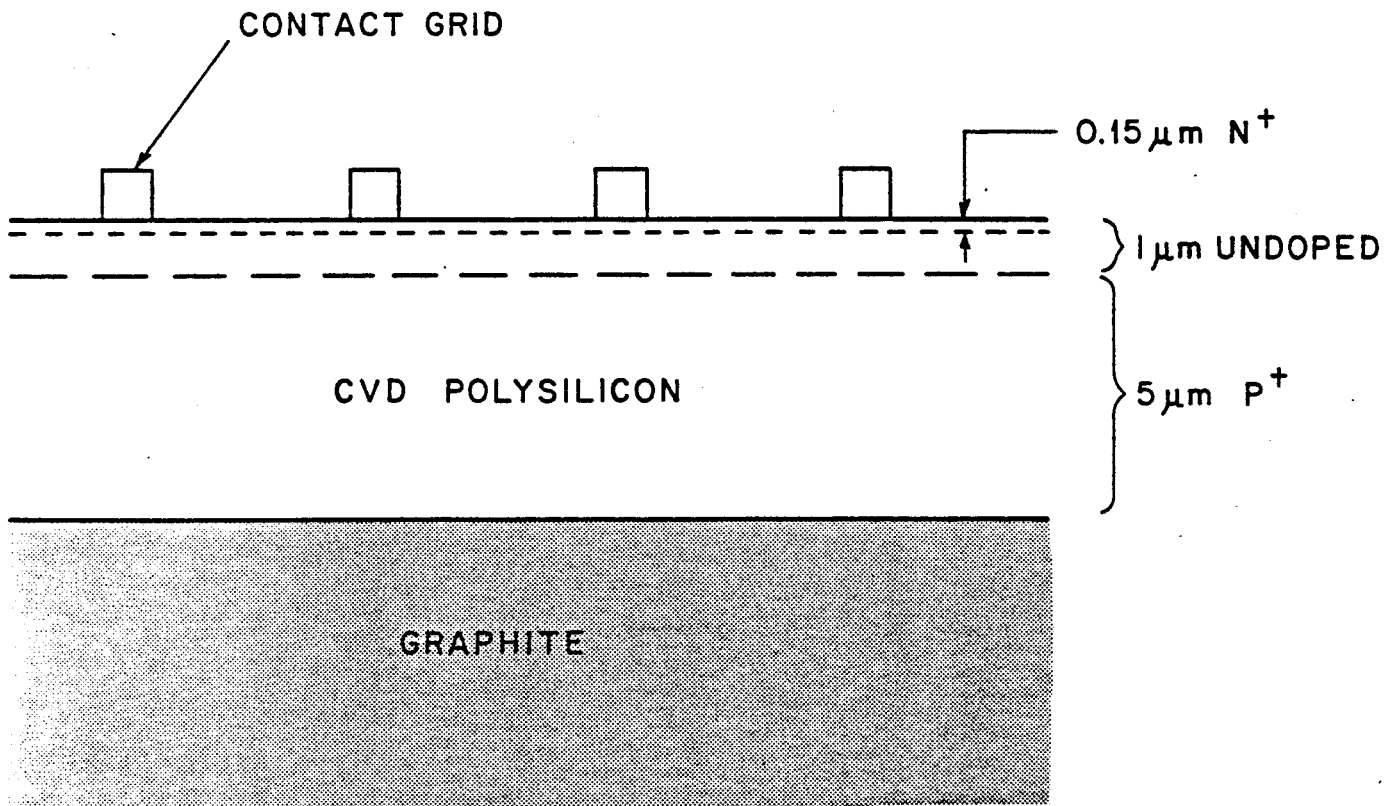


FIGURE 24. AMORPHOUS SILICON CELL STRUCTURE

It was hoped that the structure utilized might allow an amorphous layer introduced by $^{28}\text{Si}^+$ ion implantation to fall primarily in relatively lightly doped silicon below the shallow junction. Contamination of the cell zone silicon by outdoping from the 5 microns of boron doped silicon below and by foreign impurities from the graphite were unavoidable and of unknown concentration. It was found that the somewhat coarse surface on the graphite caused an irregular silicon film surface which resulted in discontinuous shallow junctions and all resulting cells had low shunt resistances and low open circuit voltages.

Figure 25 shows the AM0 I-V characteristic of Cell A which did not have $^1\text{H}^+$ or $^{28}\text{Si}^+$ implants, of cell C, with $3 \times 10^{16} \text{ } ^1\text{H}^+$ ions/cm², and of cell D, with $3 \times 10^{16} \text{ } ^1\text{H}^+$ ions/cm² plus $^{28}\text{Si}^+$ for amorphization. The simple polycrystalline film cell A exhibits reasonable short circuit current density, which suggests contamination within the CVD film from the graphite could not have been unexpectedly bad. Cells with $^1\text{H}^+$ or $^{28}\text{Si}^+$ implants were not as good. The effect of only implanted hydrogen within a cell was reduced current from the cell, the largest reduction at the highest implant dose. When amorphization by $^{28}\text{Si}^+$ was included after hydrogen implantation, cell outputs were further reduced. At a lower hydrogen dose, as in cell D shown in Figure 25, cells showed some output, but at higher hydrogen doses the cells with $^{28}\text{Si}^+$ amorphization did not exhibit photovoltaic outputs.

The I-V characteristics of the cells with higher hydrogen doses and $^{28}\text{Si}^+$ amorphization exhibited unusual behavior in that they were different when plotted slowly by manually varying a load resistance than when observed on a curve tracer. The I-V characteristics of these cells were found to be unstable and could suddenly switch between at least two different conditions. Figure 26 shows an example of a cell which could be switched back and forth between two I-V conditions by turning the illumination on or off or by increasing bias voltage to above some apparent threshold level. Figure 27 illustrates the manner in which characteristic shifts would occur when a cell was held at fixed current on a cooled test block and illumination was turned on or off. When the lamp shutter was opened the bias voltage would remain approximately stable for a period of time and then would suddenly increase substantially and restabilize. When the lamp

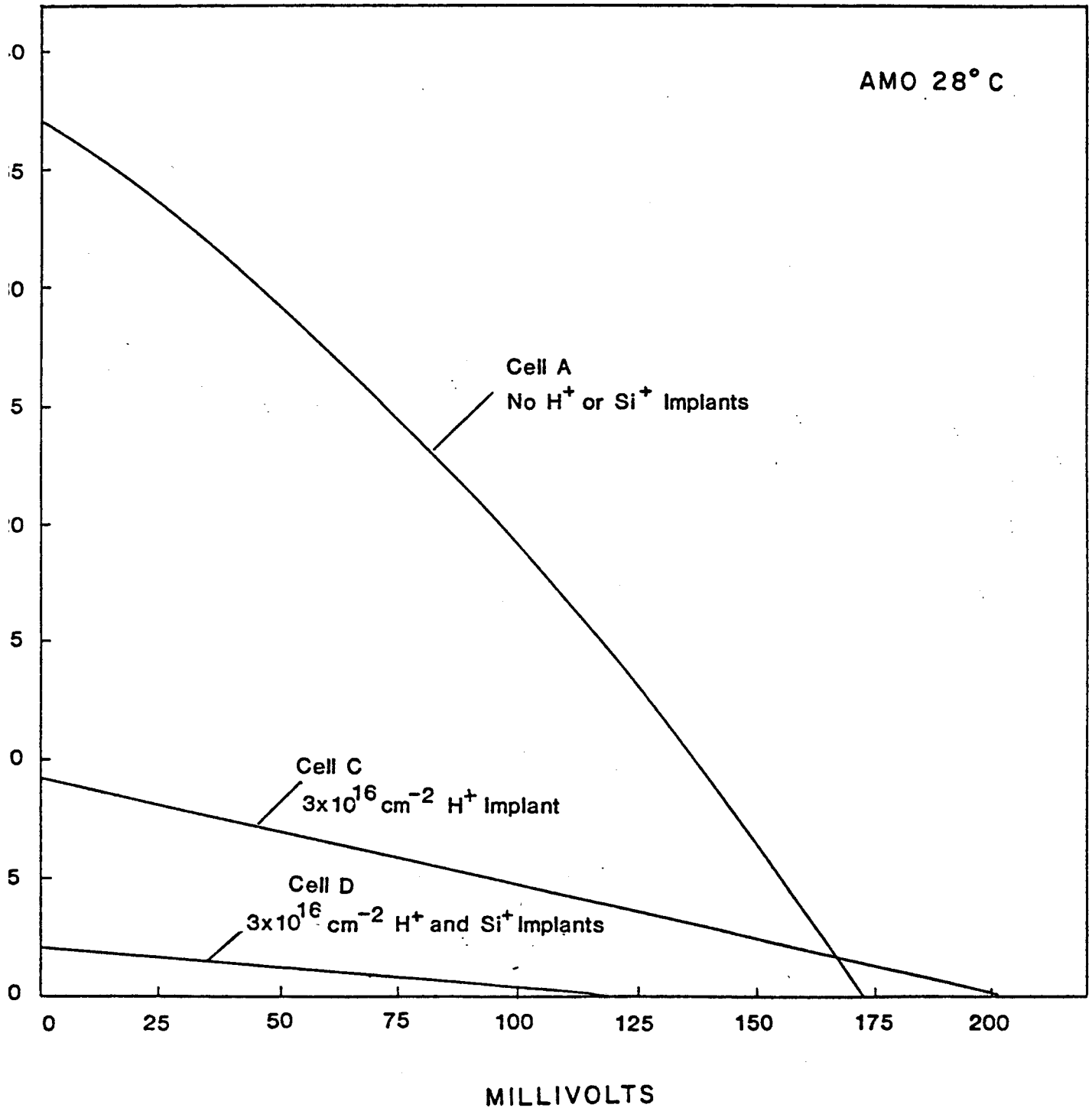


FIGURE 25. CURRENT-VOLTAGE CHARACTERISTICS OF 2x2 cm TEST CELLS

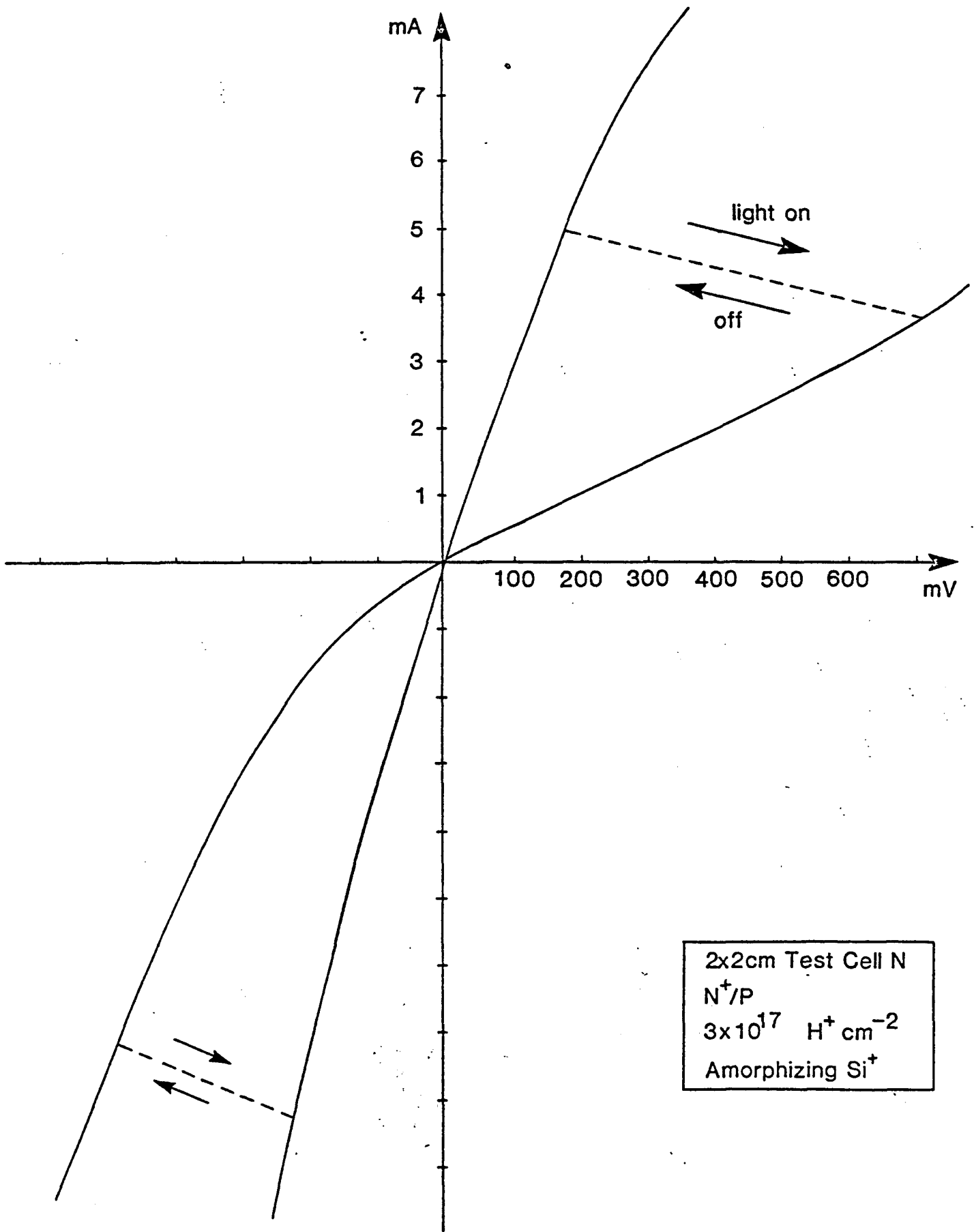


FIGURE 26. I-V CHARACTERISTICS OF UNSTABLE TEST CELL

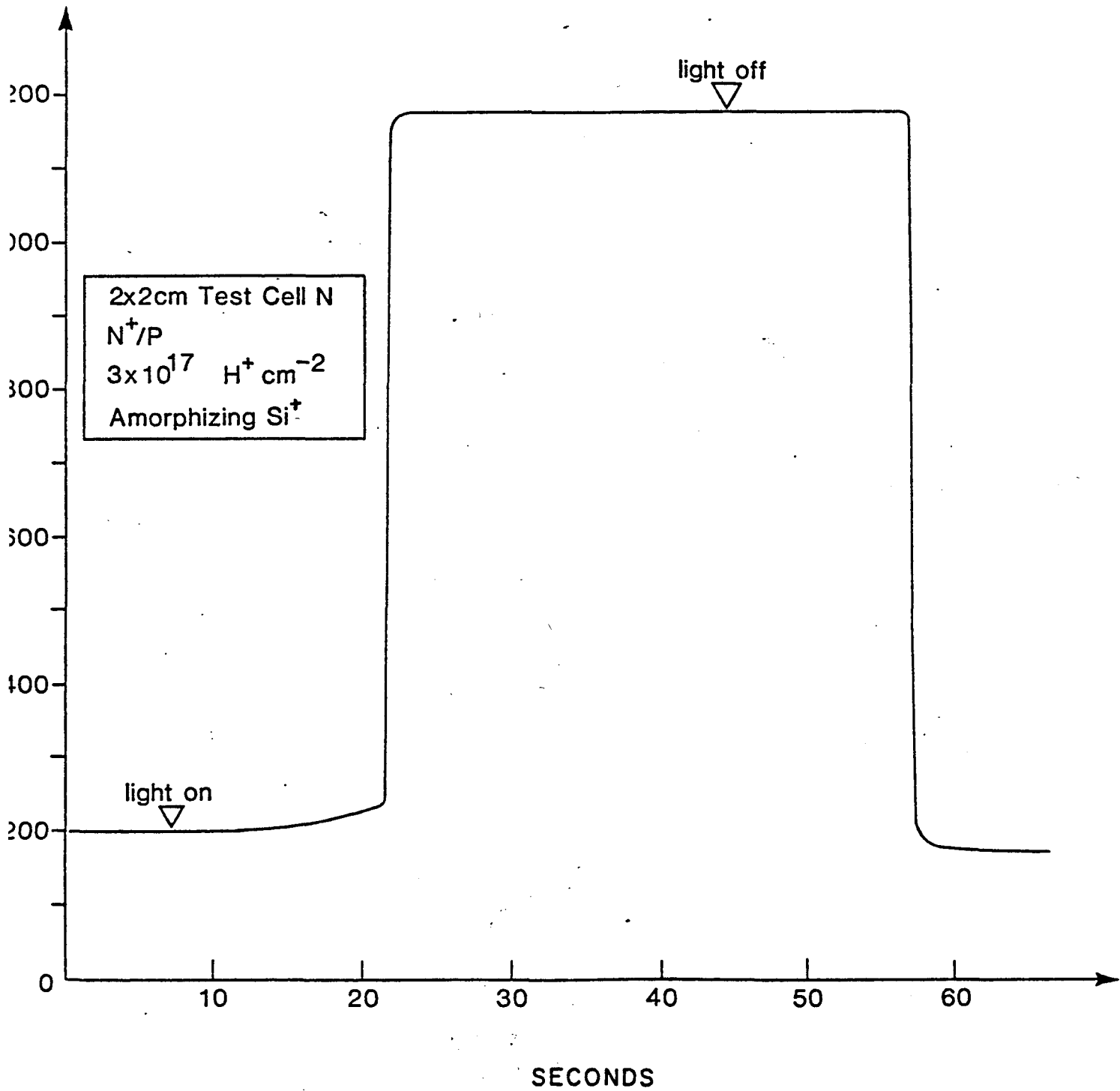


FIGURE 27. BIAS VOLTAGE AT CONSTANT CURRENT OF UNSTABLE TEST CELL

shutter was closed, the bias voltage at fixed current would after several seconds suddenly decrease to the original dark condition. This behavior was observed several times. It is believed that some internal shunting behavior must have been taking place in these cells.

Operational 2 x 2 cm amorphous silicon solar cells did not result from the attempt to fabricate such units. The information needed to select an adequate structure for such a device is believed to not yet exist. It is clear that to make such a cell using high temperature CVD to deposit a silicon film onto a substrate will be extraordinarily difficult because of problems involving inability to provide a back contact without poisoning the deposited silicon.

SECTION 3 SUMMARY

At the inception of the program which has now been completed the objectives for the investigation to be conducted were to determine technical feasibility and merit of employing ion implantation techniques in the preparation of amorphous silicon film materials and ultimately in the fabrication of amorphous silicon solar cells. It is now clear that implantation can have several useful applications for preparation or modification of amorphous silicon materials and that the techniques and facilities required do not fall beyond present state-of-the-art of implantation technology. It has been shown that implantation can be used to introduce dopants, hydrogen or other constituents to where they are needed and in concentrations desired. It has been shown that polycrystalline or crystalline silicon can be converted by ion implantation into a direct bandgap amorphous material, and it has also been shown that implantation techniques can be used to modify the optical and electrical properties of the material produced. Functional, although unsatisfactory, simple cell devices of amorphous material prepared using implantation have been accomplished.

Under the program special implantation techniques and procedures for amorphous silicon were developed, the range of effects which can be considered have been examined and useful analytical tools have been identified. Basic effects of $^1\text{H}^+$ and $^{28}\text{Si}^+$ implantation on the optical properties and electrical behavior of silicon films have been determined.

Much remains to be learned, particularly relative to basic process kinetics, relative to controlling rather than simply effecting the modifications which can be produced by implantation and relative to identifying necessary physical composition and structure of amorphous cell devices which should be addressed by exploiting implantation capabilities. Obvious near term uses of implantation for amorphous materials do however exist. Amorphous silicon films prepared by the standard method now in use could be advantageously modified by employing implantation to adjust hydrogen concentration and distribution and to add type dopants or special impurities such as fluorine in controlled quantities. Implantations utilized in this manner could represent an extremely powerful tool in determining the structural and compositional characteristics needed to improve cell performance to beyond present limits.